

1 **Comammox *Nitrospira* bacteria outnumber canonical nitrifiers irrespective of electron**
2 **donor mode and availability.**

3
4 Katherine J. Vilardi¹, Irmarié Cotto¹, Maria Sevillano Rivera¹, Zihan Dai^{2,3}, Christopher L.
5 Anderson¹, Ameet Pinto⁴

6
7 ¹ Department of Civil and Environmental Engineering, Northeastern University, Massachusetts,
8 MA, USA

9 ² Key Laboratory of Drinking Water Science and Technology, Research Center for Eco-
10 Environmental Sciences, Chinese Academy of Sciences, Beijing, China

11 ³ University of Chinese Academy of Sciences, Beijing, China

12 ⁴ School of Civil and Environmental Engineering, Georgia Institute of Technology, Atlanta, GA,
13 USA.

14
15 Corresponding author email: apinto36@gatech.edu

16
17 Keywords: comammox bacteria, nitrification, drinking water biofiltration, electron donor
18
19
20
21
22
23
24
25
26
27
28
29
30
31
32
33
34
35
36
37
38
39
40
41
42
43
44
45
46

47

48 **Abstract**

49

50 Complete ammonia oxidizing bacteria coexist with canonical ammonia and nitrite oxidizing
51 bacteria in a wide range of environments. Whether this coexistence is due to competitive or
52 cooperative interactions between the three guilds, or a result of niche separation is not yet clear.
53 Understanding the factors driving coexistence of nitrifying guilds is critical to effectively manage
54 nitrification processes occurring in engineered and natural ecosystems. In this study, microcosms-
55 based experiments were used to investigate the impact of electron donor mode (i.e., ammonia and
56 urea) and loading on the population dynamics of nitrifying guilds in drinking water biofilter media.
57 Shotgun sequencing of DNA from select time points followed by co-assembly and re-construction
58 of metagenome assembled genomes (MAGs) revealed multiple clade A2 and one clade A1
59 comammox bacterial populations coexisted in the microcosms alongside *Nitrosomonas-like*
60 ammonia oxidizers and *Nitrospira-like* nitrite oxidizer populations. Clade A2 comammox bacteria
61 were likely the primary nitrifiers within the microcosms and increased in abundance over canonical
62 ammonia and nitrite oxidizing bacteria irrespective of electron donor mode or nitrogen loading
63 rates. This suggests that comammox bacteria will outnumber nitrifying communities sourced from
64 oligotrophic environments irrespective of variable nitrogen regimes. Changes in comammox
65 bacterial abundance were not correlated with either ammonia or nitrite oxidizing bacterial
66 abundance in urea amended systems where metabolic reconstruction indicated potential cross
67 feeding between ammonia and nitrite oxidizing bacteria. In contrast, comammox bacterial
68 abundance demonstrated a negative correlation with that of nitrite oxidizers in ammonia amended
69 systems. This suggests that potentially weaker synergistic relationships between ammonia and
70 nitrite oxidizers might enable comammox bacteria to displace nitrite oxidizers from complex
71 nitrifying communities.

72 **Importance**

73 A deeper understanding of the interactions between nitrifying microorganisms, including
74 comammox bacteria, is crucial to effectively managing nitrogen in engineered and natural systems.
75 Despite their ubiquitous detection, our understanding of interactions between these coexisting
76 nitrifying groups is limited. Here, we investigate the influence of differing sources of electron
77 donor and loadings on a mixed nitrifier community which includes canonical ammonia and nitrite
78 oxidizers, as well as comammox bacteria. Our results indicate that comammox bacteria will
79 dominate nitrifier communities sourced from low nitrogen environments (e.g., drinking water)
80 irrespective of fluctuations in nitrogen availability or source without directly competing with
81 canonical ammonia oxidizers. However, canonical nitrite oxidizers are likely to get outcompeted
82 by comammox bacteria in situations where metabolic interactions between ammonia and nitrite do
83 not include cross feeding.

84

85 **Introduction**

86
87 Nitrification, the biological transformation of ammonia to nitrate via nitrite, is an important process
88 in engineered and natural ecosystems. While nitrification mediated by ammonia oxidizing
89 microorganisms (AOM) (1, 2), including ammonia oxidizing bacteria (AOB) and archaea (AOA),
90 and nitrite oxidizing bacteria (NOB) (3) has been extensively investigated, complete ammonia
91 oxidation (comammox) performed by comammox bacteria is understudied in large part due to its
92 recent discovery. All known comammox bacteria belong to *Nitrospira* sub-lineage II (4-6) and are
93 currently divided into two clades, A and B, with clade A further separated into sub-clades A1 and
94 A2 (7). Due to close phylogenetic relatedness, comammox-*Nitrospira* cannot be distinguished
95 from *Nitrospira*-NOB based on the 16S rRNA gene sequence or the marker genes for nitrite
96 oxidation (*nxrAB*) (4). Thus, characterization of comammox bacteria has been largely enabled by
97 shotgun DNA sequencing followed by reconstruction of assembled genomes (6, 8-12) and the
98 development of primers targeting subunit of comammox bacteria ammonia monooxygenase
99 (*amo*) gene (13-18).

100

101 Within the engineered water cycle, clade A1 comammox bacteria have been primarily detected in
102 wastewater treatment plants while clade A2 and B are been associated with drinking water
103 treatment and distribution systems (7). It is unclear if this translates into physiological differences
104 between the clades/sub-clades since there is only one comammox isolate and an enrichment
105 enrichments whose kinetics have been characterized. To date, kinetic parameters of comammox
106 bacteria are confined to two clade A representatives, cultured *Candidatus N. inopinata* and an
107 enrichment of *Candidatus N. kreffii* (19, 20). Both demonstrate a high affinity for ammonia, with
108 half-saturation constants orders of magnitude lower than strict AOB. Comparatively, the

109 *Candidatus* N. kreffti enrichment exhibited a higher affinity for nitrite compared to *Candidatus* N.
110 inopinata and partial inhibition of ammonia oxidation even at low ammonia concentrations (20).
111 This suggests that clade-specific comammox bacterial niche, if applicable, may be arise from a
112 combination of factors ranging from affinity to inhibition. Beyond clade specific traits, identifying
113 the potential environmental and physiological factors driving the coexistence of comammox
114 bacteria with canonical nitrifiers is also important to better understand comammox bacteria role in
115 complex nitrifying communities (21-29). Comammox bacteria have been detected along with their
116 canonical nitrifying counterparts in wastewater treatment plants (18, 25, 30-32), drinking water
117 systems (6, 9, 15, 33, 34) and soils (22, 28, 35, 36) at varying abundances over a wide range of
118 ammonium concentrations. While there is currently no quantitative estimate of the contribution of
119 comammox bacteria to nitrification compared to AOB and NOB, several studies have investigated
120 comammox bacterial dynamics in the context of mixed nitrifying communities. For instance,
121 DNA/RNA stable isotope probing combined with transcriptional analysis provided support for
122 comammox *Nitrospira* contributing to ammonia oxidation in lab-scale biofilters exposed to very
123 low ammonium concentrations (21). Soil microcosm amended with high ammonia concentrations
124 were enriched in AOB compared to those with lower ammonia concentrations where clade B
125 comammox bacteria proliferated (24, 28). Interestingly, in a lab-scale partial nitrification-
126 anammox reactor operating with incrementally increased ammonia loadings, comammox bacteria
127 initially dominated over strict AOB but its abundance significantly declined as loadings were
128 further increased (29).

129

130 Comammox bacteria may also acquire ammonia via urea degradation. Specifically, genes
131 encoding for urea transport and the urease enzyme are distributed among many *Nitrospira*

132 populations (37), including most comammox populations (38). While this may diversify potential
133 nitrogen sources for comammox bacteria (3), this could be a potential advantage for canonical
134 nitrifiers involved in a reciprocal feeding strategy as observed with co-cultured *Nitrospira*
135 *moscoviensis* converting urea to ammonia for *Nitrosomonas europaea* (37). The tight interplay
136 between canonical nitrifiers is well established; however, our understanding of comammox
137 competition (or lack thereof) with AOM and its impact on strict NOB in mixed communities is
138 limited. To better understand the comammox bacterial role within these complex nitrifying
139 communities, we investigated their population dynamics across two electron donor modes
140 (ammonia or urea) at three total nitrogen dosing strategies. The objectives of this study were (1)
141 to determine if comammox bacteria and canonical nitrifiers exhibit concentration and nitrogen
142 source dependent dynamics when subject to repeat nitrogen amendments and (2) to determine if
143 these dynamics are consistent or variable at the clade or population within each functional guild.

144

145 **Results**

146 **Microbial community composition in microcosms and nitrogen biotransformation potential.**

147 Microcosms consisting of granular activated carbon (GAC) from drinking water biofilters were
148 subject to intermittent amendments of nitrogen using two sources of electron donor (ammonia or
149 Urea) across three nitrogen concentrations (14, 3.5, and 1.5 mg-N/L). The conditions used in these
150 experiments are denoted as 14A, 3.5A, 1.5A, 14U, 3.5U and 1.5U where A or U represents
151 ammonia or urea amendments, respectively, and the number represents the concentration of
152 electron donor spike in mg/L as nitrogen. Two microcosms were sacrificed on a weekly basis over
153 the duration of a eight week experiment (n=96 total microcosms). Extracted DNA from the inocula
154 and weeks four and eight were subject to shotgun DNA sequencing (n=13).

155 Initial assessment of taxonomic diversity in the samples based on analyses of metagenomic reads
156 mapping to the small subunit rRNA database (SILVA SSU NR99 version 138.1) indicated that the
157 GAC inocula largely consisted of bacteria with archaea and eukaryota constituting a small
158 proportion of the overall metagenomic reads (~0.002%). The bacterial community was primarily
159 composed of Gammaproteobacteria (30-20%), Alphaproteobacteria (25-31%) and Nitrospirota (8-
160 15%) (Figure 1A). *Nitrospira* and *Nitrosomonadaceae* were the only nitrifiers identified and
161 constituted 9-15% of the overall microbial community in samples. Full length 16S rRNA gene
162 sequences were assembled from each sample (n=13) resulting in a total of eight sequences with
163 closest matching SILVA database hits to uncultured *Nitrospira* bacteria (Accession numbers:
164 MF040566, AY328760, JN868922). Clustering of all eight *Nitrospira* 16S rRNA gene sequences
165 at 99% identity resulted in two *Nitrospira* operational taxonomic units (OTUs) with one cluster
166 composed of six sequences (*Nitrospira* OTU 1) and the other cluster with two sequences
167 (*Nitrospira* OTU 2). Phylogenetic placements of these OTUs revealed both clustered within
168 *Nitrospira* sublineage II (supplementary figure S1A). Diversity of *Nitrospira* was likely
169 underrepresented as full length *Nitrospira* 16S rRNA gene sequences could not be assembled from
170 some samples despite a large portion of extracted 16S rRNA gene reads mapping to *Nitrospira*
171 references in the SILVA database. Limited assembly of these reads could be due to several closely
172 related *Nitrospira* species/strains coexisting in the samples making re-construction of full length
173 sequences difficult. For canonical AOB, *Nitrosomonas* sp. AL212 (CP002552) was the closest
174 matching database hit to one assembled sequence while another six had hits closet to
175 *Nitrosomonadaceae* (Accession numbers: FPLP01009519, KJ807851, FPLK01002446) but could
176 not be further classified at the genus or species level. Phylogenetic placement of the single

177 Nitrosomonas OTU affiliated it with *Nitrosomonas* sp. AL212 and *Nitrosomonas ureae* (Figure
178 S1B).

179

180 Following co-assembly of metagenomic reads, predicted protein coding genes from scaffolds
181 associated with the nitrogen metabolism were taxonomically classified (Figure 1B). The majority
182 of methane/ammonia monooxygenase (*pmo-amo*) like genes (KEGG orthology: K10944, K10945,
183 K10946) were associated with either nitrifiers (i.e., *Nitrospira* or *Nitrosomonas*) or methanotrophs
184 (i.e., *Methylocystis*) (Figure 1C). While some *amoCAB* genes could not be classified to the genus
185 level using kaiju software, blastp searches against the NCBI non-redundant protein database
186 indicated these were closely related to *Nitrosomonas*. All retrieved *hao* sequences (KEGG
187 orthology: K10535) were associated with *Nitrospira* which is likely due to the low relative
188 abundance of *Nitrosomonas*-like populations and the resulting inability to assemble their *hao*
189 genes. Potential for ureolytic activity was detected across four phyla based on the urease alpha
190 subunit (*ureC*). *ureC* sequences associated with Nitrospirota and Gammaproteobacteria could be
191 classified at the genus level as *Nitrospira* and *Nitrosomonas*. Sequences identified as nitrate
192 reductase/nitrite oxidoreductase alpha and beta subunits (K00370, K00371) were subject to further
193 classification to differentiate between nitrite oxidoreductase genes belonging to NOB from nitrate
194 reductases belonging to other community members. Phylogenetic placement of most *Nitrospira*
195 *nxrA* sequences found in this study cluster within a branch containing both comammox and
196 *Nitrospira*-NOB species (Candidatus *N. inopinata*, Candidatus *N. nitrosa* and *N. defluvii*) (Figure
197 1D). While other sequences clustered on a separate branch with Candidatus *N. nitrificans*, a single
198 *Nitrospira nxrA* sequence clustered closely within a branch containing only *Nitrospira*-NOB
199 belonging to sublineage II.

200

201

202 **Phylogenomic placement of nitrifying populations and their metabolism.**

203 To further define the composition of nitrifiers, metagenome assembled genomes (MAGs) were
204 obtained from GAC microcosms after dereplication of MAGs from three binning approaches. All
205 204 MAGs were classified as bacteria, with 145 MAGs exhibiting completeness greater than 70%
206 and contamination less than 10% (Table S1). Approximately 62% of the metagenomic reads
207 mapped to these MAGs. Nine MAGs in total were classified as nitrifying bacteria belonging to
208 *Nitrosomonas* and *Nitrospira* (Table S2). Genome annotation confirmed that four *Nitrospira*
209 MAGs had key ammonia (ammonia monooxygenase and hydroxylamine oxidoreductase) and
210 nitrite (nitrite oxidoreductase) oxidation genes (Figure S2). Quality assessment for these
211 comammox MAGs indicated two high (Bin_49_2_2 and Bin_49_4) and one medium quality
212 (Bin_260) (Table S1) according to (39). A fourth comammox MAG (Bin_13) was assembled with
213 high completeness (89%) but also possessed high redundancy (18%) that could not be improved
214 with further manual refinement. The remaining two *Nitrospira* MAGs (Bin_7_1 and Bin_188),
215 which were likely strict NOB due to lack of ammonia oxidation genes, were less complete (38.04%
216 and 48.25%) with low redundancy (8.76% and 8.46%). The low completeness was likely not due
217 to their lower abundance, but potentially high level of strain heterogeneity which may have
218 affected the assembly of reads associated with *Nitrospira*-NOB. For example, RPKM-based
219 relative abundance estimated using all reads (total RPKM) showed the two *Nitrospira*-NOB
220 MAGs exhibited similar relative abundance to comammox bacteria MAGs Bin_49_2_2 and
221 Bin_49_4 (~7-10 total RPKM), but the CheckM estimated strain heterogeneities for Bin_7_1 and
222 Bin_188 were 40 and 75, respectively, compared to 0 for both Bin_49_2_2 and Bin_49_4. Two

223 MAGs classifying as *Nitrosomonas* were deemed high (Bin_83) and medium quality (Bin_168);
224 however, a third *Nitrosomonas* MAG was considered low quality.

225 A maximum likelihood tree based on 91 single copy core genes confirmed all *Nitrospira* MAGs
226 affiliated with sublineage II (Figure 2A). Four of the *Nitrospira* MAGs from this study clustered
227 within clade A comammox *Nitrospira* (Bin_49_2_2, Bin_49_4, Bin_260 and Bin_13) but were
228 separated into distinct groups on the phylogenomic tree; namely, forming three clusters with
229 MAGs obtained from tap water, drinking water filters, and freshwater. *amoA*-based phylogenetic
230 analysis corroborated their placement into clade A (Figure 2B); however, *hao*-based phylogeny
231 distinguished three of comammox MAGs (Bin_49_2_2, Bin_49_4, Bin_260) as clade A2 (Palomo
232 et al. 2019) while one clustered within clade A1 (Bin_13) (Figure 2C). Consistent across all trees,
233 Bin_49_2_2 and Bin_260 cluster closely with comammox MAGs *Nitrospira* sp. SG-bin2 and ST-
234 bin4 (ANI ~ 92%) derived from tap water metagenomes (9). Bin_49_4 clustered closely with
235 *Nitrospirae* bacterium Ga0074138 (ANI ~ 99%), which was previously detected in GAC from the
236 same drinking water treatment plant (6), along with other tap water and groundwater-fed rapid
237 sand filter MAGs (8, 9). Bin_13 associated with comammox MAGs obtained from freshwater,
238 UBA5698 and UBA5702 (40) (ANI ~ 90%); however, its high contamination (18%) likely renders
239 ANI comparison less accurate. Overall, the MAGs demonstrated less than 95% ANI to other
240 reference comammox bacterial MAGs (Figure S3) suggesting comammox bacteria detected in
241 GAC microcosms are distinct from one another and previously published comammox MAGs; as
242 a result, they are likely novel *Nitrospira* species. The two remaining *Nitrospira* MAGs, Bin_7_1
243 and Bin_188, clustered with strict *Nitrospira*-NOB MAGs recovered from tap water,
244 *Nitrospira* sp_ST-bin5 (9) (ANI ~ 94%), and a rapid sand filter, *Nitrospira* CG24D (ANI ~ 87%)
245 (8) (Figure 2A and S3). Only two strict AOB MAGs (Bin_83 and Bin_168) from this study were

246 used for phylogenomic analysis due high redundancy and low completeness of the third (Bin_195).
247 Both Bin_83 and Bin_168 originate from *Nitrosomonas* cluster 6a and clustered closely with
248 *Nitrosomonas ureae* and *Nitrosomonas* sp. AL212 (Figure 2D). Bin_168 shares a high sequence
249 similarity to *N. ureae* (ANI ~ 98%) while Bin_83 shares less than 83% ANI to any of the references
250 on the tree including Bin_168.

251
252 All comammox MAGs demonstrated the potential for ureolytic activity with the presence of the
253 *ureABC* operon in addition to most genes for urease accessory proteins (Figure S2). *Nitrospira*-
254 NOB MAGs did not contain genes encoding for urease; however, two *ureC* sequences found on
255 assembled scaffolds that were classified as *Nitrospira* but were not binned into any of the
256 *Nitrospira* MAGs. Queries of these *ureC* genes against the NCBI non-redundant database revealed
257 one sequence shared the highest percent identity to *Nitrospira lenta* and *Nitrospira moscoviensis*
258 while top hits for the second sequence belonged to an unclassified *Nitrospira*. One *Nitrospira*-
259 NOB MAG (Bin_7_1) did harbor genes for the urea transport system permease proteins (*urtBC*),
260 urea transport system substrate-binding proteins (*urtA*) and urea transport system ATP-binding
261 proteins (*urtDE*). This suggests that the two unbinned *ureC* genes likely belonged to *Nitrospira*-
262 like NOB bacteria. *Nitrosomonas* MAGs Bin_168 and Bin_83 each contained the *ureCAB* operon
263 and some genes for urease accessory proteins and urea transport. A third *ureC* sequence found in
264 the metagenome classified as *Nitrosomonas* but was not binned into any *Nitrosomonas* MAGs.

265

266 **The impact of nitrogen amendments on nitrifying populations.**

267 To address concentration and nitrogen source-dependent dynamics of the three nitrifier
268 populations detected in our metagenomic analysis, qPCR-assays were used to estimate their

269 abundances over time in the nitrogen amended microcosms. In the high ammonia amendment
270 (14A), strict AOB relative abundance increased 2.4-fold from weeks 1-3 but remained below 2%
271 of total bacteria for the duration of the experiment whereas comammox relative abundance
272 increased markedly over time reaching 2.8% of total bacteria by end of the experiment (Figure
273 3B). Similar to strict AOB, *Nitrospira*-NOB relative abundance increased early on but thereafter
274 reduced from 4% at its peak in week two to 1.8% by week eight. Weekly measurements for
275 nitrogen concentrations taken alongside biomass samples indicated the presence of residual
276 ammonia and accumulated nitrite concentrations were highest during the first three weeks of the
277 experiment but gradually reduced over time with most inorganic nitrogen present as nitrate (Figure
278 S4). While comammox bacteria were always dominant, the abundance of strict AOB as a portion
279 of AOM was significantly higher when ammonia and nitrite accumulated in weeks 1-3 as
280 compared to weeks 5-8 (Welsh's t-test, p-value < 0.05) (Figure 3A).

281

282 The qPCR data was in concordance with metagenomic estimation of MAG abundance with clade
283 A2 comammox (Bin_49_2_2, Bin_49_2 and Bin_260) highly abundant compared to strict AOB
284 (Bin_83, Bin_168 and Bin_195) and clade A1 comammox (Bin_13) in the inocula and at weeks
285 four and eight in the high ammonia amendment (Figure 3C). In particular, clade A2 MAGs
286 Bin_49_2_2 and Bin_49_4 were the most dominant comammox populations while strict AOB was
287 dominated by Bin_83 at each time point. *Nitrospira*-NOB MAGs had comparable abundance to
288 clade A2 comammox MAGs but displayed limited variation in abundance in the high ammonia
289 amendments. This contrasts with the qPCR data, where *Nitrospira*-NOB were significantly more
290 abundant than comammox bacteria at earlier timepoints and then demonstrated a significant
291 decrease in abundance over time. This is likely due to the fact that the two assembled *Nitrospira*-

292 NOB MAG's do not represent the entirety of NOB diversity in the microcosms and the fact that
293 metagenomic data is only available for select timepoints as compared to qPCR data.
294 Nitrifier populations in mid and low ammonia amendments displayed similar dynamics to those
295 observed in high ammonia with comammox relative abundance increasing to 3% and 2.2% of total
296 bacteria by week eight, respectively. Interestingly, Bin_260, the least abundant clade A2
297 comammox MAG in the inocula, demonstrated significant increase in abundance in the low
298 ammonia amendment over the course of the experiment compared to its abundance in the other
299 ammonia amendments. Consistent with the ammonia amended microcosms, strict AOB in urea
300 amended microcosms increased in relative abundance only at earlier time points followed by low
301 but stable relative abundance (~2% of total bacteria). In the high urea amendment, relative
302 abundance of comammox bacteria remained largely unchanged at earlier time points followed by
303 an increase in abundance. Despite this, mean relative abundance of comammox bacteria compared
304 to strict AOB was still approximately 2-fold greater in all urea amendments. Similar to the
305 ammonia amendments, *Nitrospira*-NOB relative abundance did increase initially followed by a
306 decline in all urea amendments. Interestingly though, the relative abundance of comammox
307 bacteria and *Nitrospira*-NOB were similar in the later weeks of the experiment after *Nitrospira*-
308 NOB's initial rise in urea amendments. Clade A2 comammox MAG Bin_260 was consistently
309 lower in abundance than Bin_49_2_2 and Bin_49_2 in the urea amendments except for mid urea.
310 Abundance of the clade A1 comammox MAG remained lower than all clade A2 MAGs and
311 displayed minimal enrichment in all the urea amendments which was consistent with ammonia
312 amended microcosms. Bin_168, which showed high sequence similarity to *Nitrosomonas ureae*,
313 did not exhibit enrichment in any of the urea amendments and remained low in abundance with all
314 other strict AOB MAGs.

315

316 There was no significant difference in mean relative abundance of strict AOB or *Nitrospira*-NOB
317 between the high ammonia (14A) and urea amendments (14U) (Welch t-test, $p > 0.05$) but the
318 mean relative abundance of comammox bacteria was significantly greater in high ammonia than
319 in the high urea amendment (Welch t-test, $p < 0.05$). Comparatively, out of all nitrogen
320 amendments, mean relative abundance of comammox bacteria was the lowest in high urea (1.8%
321 of total bacteria). Comparisons between the mid ammonia (3.5A) and urea amendments (3.5U) as
322 well as the low ammonia (1.5A) and urea (1.5U) amendments revealed no significant difference
323 in mean relative abundance for any of the nitrifier populations (Welch t-test, $p > 0.05$).
324 Additionally, no significant differences were detected when testing the mean relative abundance
325 of the three nitrifier populations between high, mid, and low concentrations within each
326 amendment type (ANOVA, $p > 0.05$).

327

328

329 The relative abundance of the nitrifying groups were used to examine potential correlations
330 between the different populations in each of the nitrogen amendments. The ratio of comammox
331 bacteria as portion of AOM to comammox bacteria as a portion of total *Nitrospira* revealed a
332 strong positive relationship in all amendments (Pearson $R = 0.75-0.87$, $p < 0.001$) (Figure S5A),
333 however, the change in relative abundance of comammox bacteria was not directly correlated with
334 that of strict AOB in any of the nitrogen amendments (Figure S5B). Strict AOB and *Nitrospira*-
335 NOB abundances were strongly correlated for all urea amendments and high (14A) and mid
336 ammonia (3.5A) (Pearson $r = 0.58-0.82$, $p < 0.05$, Figure 4A) but exhibited a weaker relationship
337 in low ammonia (Pearson $r = 0.42$, $p > 0.05$). Interestingly, while comammox bacteria abundance
338 was significantly and negatively correlated with that of *Nitrospira*-NOB in ammonia amendments

339 (Pearson $r = -0.37$ to -0.61) ($p < 0.05$), there was no significant association between them in the
340 urea amendments ($p > 0.05$) (Figure 4B).

341
342

343 **Discussion**

344 **Key nitrifiers encompassing *Nitrospira* and *Nitrosomonas*-like bacteria share ureolytic** 345 **potential**

346
347 16S rRNA gene sequences assembled from short reads indicated *Nitrospira*- and *Nitrosomonas*-
348 like populations were the only nitrifiers present in the microcosms. The proportion of 16S rRNA
349 gene reads mapping to *Nitrospira*-like populations in this study suggested that they were highly
350 abundant in the inocula and nitrogen amendments. Surveys of other DWTP biofilters using 16S
351 rRNA gene amplicons have indicated that sublineage II *Nitrospira* account for a dominant portion
352 of the bacterial community (41) with further investigation confirming high contributions to its
353 abundance were from comammox-*Nitrospira* (8, 33). The strict AOB OTU found in this study was
354 affiliated with oligotrophic *Nitrosomonas* cluster 6a which exhibit maximum growth rates at
355 ammonia concentrations similar to the ones used for high and mid nitrogen amendments (42, 43).
356 Despite this, the proportions of SSU reads mapping to *Nitrosomonas*-like populations in all
357 nitrogen amendments were consistently low. Taxonomic classification of nitrogen cycling genes
358 revealed metabolic potential for nitrification processes were confined to *Nitrospira*- and
359 *Nitrosomonas*-like populations corroborating with assembled 16S rRNA gene sequences.
360 Additionally, phylogeny of *amoA* sequences found in the metagenome indicated ammonia
361 oxidation could be mediated by both *Nitrospira* and *Nitrosomonas*. Consequently, nitrate made
362 available from nitrification processes would be available for nitrate reduction by other community
363 members or as a source of nitrogen for biomass synthesis in oligotrophic environments.

364

365 We assembled a total of nine nitrifier MAGs which included comammox-*Nitrospira* (n=4),
366 *Nitrospira*-NOB-like (n=2), and *Nitrosomonas*-like (n=3) populations. Three of the four
367 comammox MAGs assembled were identified as clade A2 based on phylogenetic analyses of
368 hydroxylamine dehydrogenase (*hao*) which has previously been shown to dominate drinking water
369 biofilters along with comammox clade B (7). The remaining comammox MAG assembled from
370 biofilter media in this study was affiliated with clade A1 based on *hao* gene phylogeny, which
371 while atypical for drinking water biofilters is consistent with previously published metagenome
372 from the Ann Arbor drinking water filters (6). Similar coexistence of clade A1 and A2 comammox
373 bacteria with canonical nitrifiers has been observed in tertiary rotating biological contactors
374 treating municipal wastewater with low ammonium concentrations (44). However, phylogenomic
375 placement of clade A sub-groups in this study separated the comammox MAGs into distinct
376 clusters associated with freshwater (Bin_13, clade A1), groundwater biofilters (Bin_49_4, clade
377 A2) and tap water (Bin_260 and Bin_49_2_2, clade A2). Maintenance of high functional
378 redundancy for the complete ammonia oxidation pathway may rely on coexisting comammox
379 populations avoiding direct competition through distinct physiological niches. Additionally, the
380 inocula were sourced from low substrate conditions which may also allow for the coexistence of
381 multiple comammox populations. Strict AOB MAGs obtained in this study associated with low
382 ammonia adapted *Nitrosomonas* cluster 6a (45) which is consistent with the inocula source being
383 an oligotrophic environment (i.e., DWTPs). Furthermore, close relatives of *Nitrospira*-NOB
384 MAGs obtained in this study originated from a tap water source where *Nitrospira*-NOB also
385 coexisted with strict AOB and comammox bacteria under oligotrophic conditions (9). Our
386 findings, consistent with previous studies, confirm the nitrifier community encompassed multiple
387 populations capable of single and two-step nitrification within a single system. Further, assessment

388 of metabolic versatility revealed initiation of nitrification through urea degradation was possible by
389 all three nitrifying guilds. Though ureolytic activity is a widespread trait among cultured
390 comammox-*Nitrospira* representatives and curated MAGs, the capability is confined to only some
391 *Nitrospira*-NOB and *Nitrosomonas* species (37, 43). Here in particular, this would allow
392 *Nitrospira*-NOB to play a role in nitrite production in urea microcosms by crossing feeding
393 ammonia from urea degradation to strict AOB, a mutualistic strategy which may not be active in
394 ammonia amended microcosms.

395
396 **Comammox bacterial abundance increased irrespective of nitrogen source or loading but**
397 **may compete with NOB depending on nitrogen source type.**
398

399 We tested the impact of nitrogen source and loading rates on temporal dynamics of a mixed
400 nitrifying community to determine whether comammox bacteria are outcompeted at higher
401 concentrations and/or favored in urea amendments due to their ureolytic activity. qPCR-based
402 abundance tracking revealed comammox bacteria demonstrated a preferential enrichment over
403 strict AOB in the nitrogen amendments irrespective of electron donor source or availability.
404 Additionally, strict AOB abundance did not exhibit any significant difference across the nitrogen
405 amendment types. This is in contrast to previous work in soil microcosms where AOB abundance
406 increased in response to high ammonia amendments (28). However, strict AOB populations in
407 these soil microcosms were primarily *Nitrosospira* compared to oligotrophic *Nitrosomonas* cluster
408 6a which were the primary AOB in this study. Here, both comammox bacteria and strict AOB
409 demonstrated increased abundance in all amendments during the earlier weeks of the experiment.
410 Ultimately, while comammox bacteria were enriched over time our findings demonstrated this
411 increased abundance was not associated with a decrease in the abundance of strict AOB in any of
412 the nitrogen amendments. This suggests a lack of direct competition between the two comammox

413 and strict AOB which could be attributable to the two ammonia oxidizers occupying separate
414 nitrogen availability niches (19, 46). Stable abundances of strict AOB compared to enrichment of
415 comammox could be due to a combination of factors ranging from (1) higher abundances of
416 comammox bacteria in the inocula and (2) significantly higher biomass yields per mole of
417 ammonia oxidizers for comammox bacteria compared to AOB (19).

418

419 Clade A2 associated comammox bacterial MAGs were dominant in the inocula and over the course
420 of the experiment showed increased abundance in all amendments. In contrast, comammox
421 bacteria belonging to clade A1 were lower in abundance and did not demonstrate significant
422 change over time in any amended microcosm. Though physiological differences between
423 comammox bacteria clades/sub-clades have yet to be established, earlier studies of DWTP
424 biofilters have observed higher abundances of clade B (15) or alternatively both clades found at
425 the same DWTP but within separate rapid sand filters, where clade B was more abundant in the
426 secondary filters receiving lower ammonia concentrations (34). In this study, the lack of clade A1
427 enrichment may also indicate distinct physiological niches within clades (i.e., subclade-level niche
428 differentiation). Future research is necessary to develop a clearer understanding of physiological
429 differences between comammox bacteria at the clade/sub-clade level. Since cultivability of
430 comammox bacteria remains an ongoing challenge, integrating multiple ‘omics techniques (i.e.,
431 metatranscriptomics and metaproteomics) may be an appropriate strategy for examining ammonia
432 utilization and the expressed metabolisms of multiple coexisting comammox bacteria populations
433 alongside canonical nitrifiers.

434

435 The negative association between comammox bacteria and canonical NOB observed in ammonia
436 amendments could be a result of nitrite limitation resulting from complete nitrification driven by

437 comammox bacteria. Nitrite limitation driven competition between comammox bacteria and NOB
438 is supported by the fact the negative associations between the groups were stronger at medium (3.5
439 mg-N/l) and low (1.5 mg-N/l) nitrogen availability as compared to the high ammonia amendments
440 (i.e., 14 mg-N/l). In contrast, there was no significant association between the abundance of
441 comammox bacteria and *Nitrospira*-NOB in the urea amended systems irrespective of nitrogen
442 loading. We hypothesize that this variable observations between ammonia and urea amended
443 systems likely emerge from the extent of metabolic coupling between AOB and NOB and the
444 resultant ability of comammox to outcompete NOB. Specifically, while the rate of nitrite
445 availability for NOB in ammonia amended systems is largely dictated by ammonia oxidation
446 activity of AOB it is likely that nitrite availability in urea amended systems would be dictated by
447 a combination of both AOB activity and indirectly by NOB. In this case, the production of nitrite
448 could be mediated by *Nitrospira*-NOB capable of ureolytic activity by crossing feeding ammonia
449 to strict AOB who in turn provide nitrite at a rate at which *Nitrospira*-NOB. This tight coupling
450 between AOB and NOB is supported by stronger and more significant correlation between AOB
451 and NOB abundance in urea amended systems as compared to ammonia amended systems. Thus,
452 it appears that while comammox bacteria may outcompete *Nitrospira*-NOB in systems where AOB
453 abundances are low and nitrite availability is largely dictated by AOB activity, this competitive
454 exclusion may be limited in scenarios with established AOB-NOB cross feeding via urea where
455 nitrite availability is governed not only by AOB's ammonia oxidation rate but also by NOB's
456 ureolytic activity.

457

458 Altogether, our study demonstrates that comammox bacteria will dominate over canonical
459 nitrifiers in communities sourced from nitrogen limited environments irrespective of electron

460 donor type or loading rate without directly competing with canonical AOB. Further, our study also
461 indicates comammox bacteria and AOB may occupy independent niches in communities sources
462 from low nitrogen environments. Interestingly, we see evidence of potential competitive exclusion
463 of NOB by comammox bacteria governed by nitrogen source dependent metabolic coupling
464 between AOB and NOB.

465

466 **Materials and Methods**

467 **Experimental design and execution:** Granular activated carbon (GAC) with coexisting AOB,
468 NOB, and comammox bacterial populations from biofilters at the drinking water treatment plant
469 (DWTP) in Ann Arbor, (AA) Michigan was used as the inoculum for this experimental work (6).
470 Microcosms consisted of 3 grams of GAC supplemented with 10 mL of filter influent from AA
471 DWTP in 40 mL pre-sterilized glass vials (DWK Life Sciences – Fisher 033395C). A total of 96
472 glass microcosms were prepared such that two biological replicates for each of the three nitrogen
473 concentrations (1.5, 3.5 and 14 mg-N/L) for the two nitrogen sources (i.e., ammonium and urea)
474 were harvested weekly for analyses over the period of the 8-week experiment. Ammonium was
475 spiked in at 0.1, 0.25 and 1 mM (in the form of ammonium chloride solution), corresponding to
476 1.5, 3.5 and 14 mg-N/L. For urea, 0.05, 0.125 and 0.5 mM (in the form of urea solution) were used
477 to ensure similar concentrations of total nitrogen as the ammonium microcosms. Microcosms were
478 maintained by removing approximately 10 mL of spent filter influent and subsequently
479 replenishing them with 10 mL of fresh influent and the respective electron donor spike every two
480 days. Once a week, two microcosms per condition (i.e., nitrogen concentration and nitrogen
481 source) were sacrificed and two 0.5 g GAC samples from each microcosm were transferred to
482 Lysing Matrix E tubes (MP Biomedical Lysing Matrix E – Fisher MP116914100) and stored at -

483 80°C until further processing. Spent filter influent was filtered using 0.2 µM filtration (Sartorius
484 Minisart NML Syringe Filter – Fisher Scientific 14555269) for subsequent chemical analyses.
485 Hach Company Test n’ Tube Vials were used to determine concentrations of ammonia-N (Hach,
486 Cat No. 2606945), nitrite-N (Hach, Cat No. 2608345) and nitrate-N (Hach, Cat No. 2605345) in
487 microcosms. All samples were analyzed on a Hach DR1900 photospectrometer (Hach – DR1900-
488 01H). Alkalinity of filtered liquid samples were measured using Hach Alkalinity Total TNTplus
489 Vials (Hach – TNT870).

490

491 **DNA extraction and qPCR:** GAC samples were subjected to DNA extraction using the DNeasy
492 PowerSoil kit (Qiagen, Inc – Cat No.12888) on the QIAcube (Qiagen, Inc – Cat No. 9002160)
493 following manufacturer’s instructions with a few modifications. Specifically, the lysing buffer
494 from the PowerBead tubes were transferred to the Lysing Matrix E tubes and C1 buffer was added.
495 Prior to bead beating, an equal volume of chloroform was added (610 µL). Bead beating consisted
496 of four rounds of 40 seconds on a FastPrep-24 instrument (MP Bio – 116005500) with bead
497 beading tubes placed on ice for two minutes between each bead beating. Samples were then
498 centrifuged at 10,000 g for 1 minute and 750 µL of aqueous phase used to purify DNA using the
499 QIAcube Protocol for the DNeasy PowerSoil Kit. Each round of extractions included a reagent
500 blank as a negative control. After extraction, DNA concentration was determined using a Qubit
501 instrument with the dsDNA Broad Range Assay (ThermoFisher Scientific – Cat No. Q32850)
502 (Table S3). DNA was stored in a -80°C freezer until future use.

503

504 qPCR assays were conducted using QuantStudio 3 Real-Time PCR System (ThermoFisher
505 Scientific – Cat. No. A28567). Primer sets targeting the 16S rRNA gene of AOB (47), 16S rRNA
506 gene of *Nitrospira* (48), *amoB* gene of clade A comammox bacteria (18) and 16S rRNA gene for

507 total bacteria (49) were used (Table S4). Previously published primer set for the *amoB* gene of
508 clade A comammox bacteria was updated based on metagenomic data generated as part of this
509 study (18). Based on alignments of *amoB* gene sequences from the comammox MAGs assembled
510 in this study, the previously published forward primer for comammox clade A *amoB* from Cotto
511 et. al 2020 had one mismatch with one of our bins. Thus, this forward primer was further modified
512 by changing the 13th position from G to a degenerate base S (seven base pairs from 3'-end). The
513 use of the modified primers resulted in increased abundance of comammox bacteria in this study
514 as shown in supplementary Figure S5, indicating the ability to capture comammox *amoB* gene
515 sequences not amplified by previous primer set.

516

517 The qPCR reactions were carried out in 20 μ L volumes, which included 10 μ L Luna Universal
518 qPCR Master Mix (New England Biolabs, Inc., Cat. No. NC1276266), 5 μ L of 10-fold diluted
519 template DNA, primer concentrations are outlined in Table S4 and DNase/RNase free water
520 (Fisher Scientific, Cat. No. 10977015) to make up the remaining volume to 20 μ L. Each sample
521 per assay was subject to qPCR in triplicate and qPCR plates were prepared using the epMotion
522 M5073 liquid handling system (Eppendorf, Cat. No. 5073000205D). The cycling conditions used
523 in this study were as follows: initial denaturing at 95°C for 1 minute, 40 cycles of denaturing at
524 95°C for 15 seconds, annealing temperatures and time used are listed in Table S4 and extension at
525 72°C for 1 minute. qPCR analysis proceeded with a negative control and 7-point standard curve
526 ranging from 10^3 - 10^9 copies of 16S rRNA gene of *Nitrosomonas europaea* for total bacteria
527 quantification, 10^2 - 10^8 copies of 16S rRNA genes of *Nitrosomonas europaea* and *Ca Nitrospira*
528 *inopinata* for AOB and *Nitrospira* quantification, respectively, and $10^2 - 10^8$ copies of *amoB* gene
529 of *Ca Nitrospira inopinata* for the quantification of comammox bacteria. The primer used to detect

530 the 16S rRNA gene of *Nitrospira* would inclusively track both comammox-*Nitrospira* and
531 *Nitrospira*-NOB. Thus, *Nitrospira*-NOB abundance was estimated by subtracting the copy number
532 of comammox bacteria *amoB* from the copy number of 16S rRNA gene of *Nitrospira*.

533

534 **Metagenomic analyses:**

535 A subset of samples were selected for metagenomic analysis including DNA extracted from the
536 initial GAC inoculum and samples from weeks four and eight (n=13) for all nitrogen dosing and
537 sources. DNA extracts from duplicated microcosms for each time point were pooled by in equal
538 mass proportion before sending DNA templates for sequencing at the Roy J. Carver Biotechnology
539 Center at University of Illinois Urbana-Champaign Sequencing Core. Two lanes of Illumina
540 NovaSeq were used to generate paired-end reads ranging from 29 to 68 million per sample (2x150-
541 bp read length) (Table S5). Raw paired-end reads were trimmed and quality filtered with fastp (50)
542 (Table S5). Filtered reads were mapped to the UniVec Database (National Center for
543 Biotechnology Information) using BWA (51) to remove potential vector contamination.
544 Subsequent unmapped reads were extracted, sorted and indexed using SAMtools v1.3.1 (52) then
545 converted back to FASTQ using bedtools v2.19.1 (53).

546

547 Small subunit rRNA sequence reconstruction from quality filtered short reads was carried out
548 using the Phyloflash pipeline v3.4 (54). Briefly, bbmap was used to map short reads against the
549 SILVA 138.1 NR99 database with the default minimum identity of 70% followed by assembly of
550 full-length sequences with Spades (kmers = 99,111,127) and detection of closest-matching
551 database sequences using usearch global within VSEARCH at a minimum identity of 70%. For
552 read pairs, taxonomic classification was performed by taking the lowest common ancestor of the

553 taxonomic strings of database hits using SILVA taxonomy (55). Assembled sequences from all
554 samples belonging to nitrifying bacteria were clustered at 99% identity using vsearch v2.15.2 (56).
555 Reference *Nitrospira* and *Nitrosomonadaceae* 16S rRNA reference sequences were obtained from
556 ARB-SILVA and aligned with assembled sequences using muscle v3.8.1551 (57). Construction of
557 16S rRNA phylogenetic trees for *Nitrospira* and *Nitrosomonadaceae* was performed using IQ-
558 TREE v1.6.12 (58) with model finder option (59) selecting TIM3+F+I+G4 and TPM2u+F+I+G4
559 as models for respective trees.

560
561 Quality filtered paired-end reads from all samples were co-assembled with metaSPAdes v3.11.1
562 (60) with k-mers lengths 21, 33, 55, 77, 99, and 119, and phred off-set of 33. Quality evaluation
563 of the assembled scaffolds was performed using Quast v5.0.2 (61) (Table S6). Open reading frames
564 (ORF) on scaffolds were predicted using Prodigal v2.6.2 (62) with the “meta” flag and functional
565 prediction of resulting protein sequences were determined by similarity searches of the KEGG
566 database (63) using kofamscan (64). Taxonomic classification of scaffolds harboring nitrogen
567 cycling genes was performed using kaiju v1.7.4 (65) against the NCBI nr database with default
568 parameters. CoverM v0.5.0 (www.github.com/wwood/CoverM) was used to calculate reads per
569 kilobase million (RPKM) of these scaffolds as a metric for estimating relative abundance in each
570 sample.

571
572 Scaffolds were binned into clusters and manually refined using Anvi'o (v5.1 and 5.5) (66) with
573 three binning algorithms including CONCOCT (67), Metabat2 v2.5 (68) and Maxbin2 v2.2.7 (69).
574 DAS_tool v1.1.2 (70) was used to merge bins from the three approaches to generate final
575 metagenome assembled genomes (MAGs). Completeness and contamination of the final set was

576 determined using CheckM v1.0.7 (71) followed by taxonomic classification using the Genome
577 Taxonomy Database Toolkit v1.2.0 with release 89 v04-RS89 (72). CoverM was used to calculate
578 RPKM for each bin. Similar to the annotation of the metagenome, functional prediction of bin
579 ORFs were determined by similarity searches against the KEGG database using kofamscan. The
580 annotation of genes of interest were further confirmed by querying protein sequences against the
581 NCBI-nr database using BLASTP. MAGs were also annotated using Prokka as a secondary
582 annotation method (73). The Up-to-date Bacterial Core Gene pipeline (UBCG) (74) with default
583 parameters was used to extract and align a set of 92 single copy core genes from *Nitrospira* and
584 *Nitrosomonas* reference genomes (Table S7) and nitrifier MAGs for phylogenomic tree
585 reconstruction. Maximum likelihood trees were generated based on the nucleotide alignment using
586 IQ-TREE with model finder selecting the GTR+F+R10 and GTR+F+R4 models for *Nitrospira*
587 and *Nitrosomonas* trees, respectively, with 1000 bootstrap iterations. For outgroups, two
588 *Leptospirillum* and three *Nitrosospira* genomes were used for *Nitrospira* and *Nitrosomonas* trees,
589 respectively. Pairwise alignments of comammox *amoA* and *hao* and *Nitrospira nxrA* protein
590 sequences were created using muscle. Maximum likelihood trees were inferred by IQ-TREE with
591 model finder selecting LG+G4 for the *amoA* tree and LG+I+G4 for *hao* and *nxrA* trees with 1000
592 bootstrap iterations for each tree. The *amoA* and *hao* protein sequences from *Nitrosomonas*
593 *europaea* and *Nitrosomonas oligotropha* were used as the outgroup for comammox trees. All trees
594 were visualized using the Interactive Tree of Life (itol) (75). Pairwise comparisons of average
595 nucleotide identity of 38 *Nitrospira* and 15 *Nitrosomonadaceae* genomes (Table S4) with nitrifier
596 MAGs obtained in this study was determined using FastANI v1.31 (76).

597

598 **Statistical analysis**

599 The relative abundance of each nitrifier population was tested to determine if significant
600 differences existed between concentration or source of electron donor types using ANOVA and
601 Welch t-tests, respectively, with R version 4.0.4. Shapiro Wilks tests were used to confirm
602 normality prior to these statistical tests. Linear regression and correlation analysis were used to
603 examine the relationship between the abundance of nitrifying guilds in each of the nitrogen
604 amendments over time.

605

606 **Data availability**

607 Raw sequence reads, metagenome assembly, and MAGs are available on NCBI at Bioproject
608 number PRJNA764197.

609

610 **Funding sources**

611 This research was supported by NSF Graduate Research Fellowship and Cochrane Fellowship to
612 KV and by NSF Award number: 1703089.

613

614

615

616

617

618

619

620

621

622

623

624

625

626

627

628

629

630

631

632

633

634 References

635

- 636 1. Kowalchuk GA, Stephen JR. 2001. Ammonia-Oxidizing Bacteria: A Model for
637 Molecular Microbial Ecology. *Annu Rev Microbiol* 55:485-529.
- 638 2. Stahl DA, de la Torre JR. 2012. Physiology and diversity of ammonia-oxidizing archaea.
639 *Annu Rev Microbiol* 66:83-101.
- 640 3. Daims H, Lucker S, Wagner M. 2016. A New Perspective on Microbes Formerly Known
641 as Nitrite-Oxidizing Bacteria. *Trends Microbiol* 24:699-712.
- 642 4. Daims H, Lebedeva EV, Pjevac P, Han P, Herbold C, Albertsen M, Jehmlich N,
643 Palatinszky M, Vierheilig J, Bulaev A, Kirkegaard RH, von Bergen M, Rattei T,
644 Bendinger B, Nielsen PH, Wagner M. 2015. Complete nitrification by *Nitrospira*
645 bacteria. *Nature* 528:504-9.
- 646 5. van Kessel MA, Speth DR, Albertsen M, Nielsen PH, Op den Camp HJ, Kartal B, Jetten
647 MS, Lucker S. 2015. Complete nitrification by a single microorganism. *Nature* 528:555-
648 9.
- 649 6. Pinto AJ, Marcus DN, Ijaz UZ, Bautista-de Lose Santos QM, Dick GJ, Raskin L. 2016.
650 Metagenomic Evidence for the Presence of Comammox *Nitrospira*-Like Bacteria in a
651 Drinking Water System. *mSphere* 1.
- 652 7. Palomo A, Dechesne A, Smets BF. 2019. Genomic profiling of *Nitrospira* species reveals
653 ecological success of comammox *Nitrospira*. *bioRxiv* doi:10.1101/612226.
- 654 8. Palomo A, Jane Fowler S, Gulay A, Rasmussen S, Sicheritz-Ponten T, Smets BF. 2016.
655 Metagenomic analysis of rapid gravity sand filter microbial communities suggests novel
656 physiology of *Nitrospira* spp. *ISME J* 10:2569-2581.
- 657 9. Wang Y, Ma L, Mao Y, Jiang X, Xia Y, Yu K, Li B, Zhang T. 2017. Comammox in
658 drinking water systems. *Water Res* 116:332-341.
- 659 10. Annavajhala MK, Kapoor V, Santo-Domingo J, Chandran K. 2018. Comammox
660 Functionality Identified in Diverse Engineered Biological Wastewater Treatment
661 Systems. *Environ Sci Technol Lett* 5:110-116.
- 662 11. Poghosyan L, Koch H, Lavy A, Frank J, van Kessel M, Jetten MSM, Banfield JF, Lucker
663 S. 2019. Metagenomic recovery of two distinct comammox *Nitrospira* from the terrestrial
664 subsurface. *Environ Microbiol* 21:3627-3637.
- 665 12. Camejo PY, Santo Domingo J, McMahon KD, Noguera DR. 2017. Genome-Enabled
666 Insights into the Ecophysiology of the Comammox Bacterium "*Candidatus Nitrospira*
667 *nitrosa*". *mSystems* 2.
- 668 13. Bartelme RP, McLellan SL, Newton RJ. 2017. Freshwater Recirculating Aquaculture
669 System Operations Drive Biofilter Bacterial Community Shifts around a Stable Nitrifying
670 Consortium of Ammonia-Oxidizing Archaea and Comammox *Nitrospira*. *Front*
671 *Microbiol* 8:101.
- 672 14. Pjevac P, Schauburger C, Poghosyan L, Herbold CW, van Kessel M, Daebeler A,
673 Steinberger M, Jetten MSM, Lucker S, Wagner M, Daims H. 2017. *AmoA*-Targeted
674 Polymerase Chain Reaction Primers for the Specific Detection and Quantification of
675 Comammox *Nitrospira* in the Environment. *Front Microbiol* 8:1508.
- 676 15. Fowler SJ, Palomo A, Dechesne A, Mines PD, Smets BF. 2018. Comammox *Nitrospira*
677 are abundant ammonia oxidizers in diverse groundwater-fed rapid sand filter
678 communities. *Environ Microbiol* 20:1002-1015.

- 679 16. Wang M, Huang G, Zhao Z, Dang C, Liu W, Zheng M. 2018. Newly designed primer
680 pair revealed dominant and diverse comammox amoA gene in full-scale wastewater
681 treatment plants. *Bioresour Technol* 270:580-587.
- 682 17. Beach NK, Noguera DR. 2019. Design and Assessment of Species-Level qPCR Primers
683 Targeting Comammox. *Front Microbiol* 10:36.
- 684 18. Cotto I, Dai Z, Huo L, Anderson CL, Vilardi KJ, Ijaz U, Khunjar W, Wilson C, De
685 Clippeleir H, Gilmore K, Bailey E, Pinto AJ. 2020. Long solids retention times and
686 attached growth phase favor prevalence of comammox bacteria in nitrogen removal
687 systems. *Water Res* 169:115268.
- 688 19. Kits KD, Sedlacek CJ, Lebedeva EV, Han P, Bulaev A, Pjevac P, Daebeler A, Romano
689 S, Albertsen M, Stein LY, Daims H, Wagner M. 2017. Kinetic analysis of a complete
690 nitrifier reveals an oligotrophic lifestyle. *Nature* 549:269-272.
- 691 20. Sakoula D, Koch H, Frank J, Jetten MSM, van Kessel M, Lucker S. 2020. Enrichment
692 and physiological characterization of a novel comammox *Nitrospira* indicates ammonium
693 inhibition of complete nitrification. *ISME J* doi:10.1038/s41396-020-00827-4.
- 694 21. Gulay A, Fowler SJ, Tatari K, Thamdrup B, Albrechtsen HJ, Al-Soud WA, Sorensen SJ,
695 Smets BF. 2019. DNA- and RNA-SIP Reveal *Nitrospira* spp. as Key Drivers of
696 Nitrification in Groundwater-Fed Biofilters. *mBio* 10.
- 697 22. Liu T, Wang Z, Wang S, Zhao Y, Wright AL, Jiang X. 2019. Responses of ammonia-
698 oxidizers and comammox to different long-term fertilization regimes in a subtropical
699 paddy soil. *European Journal of Soil Biology* 93.
- 700 23. Wang J, Wang J, Rhodes G, He JZ, Ge Y. 2019. Adaptive responses of comammox
701 *Nitrospira* and canonical ammonia oxidizers to long-term fertilizations: Implications for
702 the relative contributions of different ammonia oxidizers to soil nitrogen cycling. *Sci*
703 *Total Environ* 668:224-233.
- 704 24. Wang Z, Cao Y, Zhu-Barker X, Nicol GW, Wright AL, Jia Z, Jiang X. 2019.
705 Comammox *Nitrospira* clade B contributes to nitrification in soil. *Soil Biology and*
706 *Biochemistry* 135:392-395.
- 707 25. Zheng M, Wang M, Zhao Z, Zhou N, He S, Liu S, Wang J, Wang X. 2019.
708 Transcriptional activity and diversity of comammox bacteria as a previously overlooked
709 ammonia oxidizing prokaryote in full-scale wastewater treatment plants. *Sci Total*
710 *Environ* 656:717-722.
- 711 26. Gottshall EY, Bryson SJ, Cogert KI, Landreau M, Sedlacek CJ, Stahl DA, Daims H,
712 Winkler M. 2020. Sustained nitrogen loss in a symbiotic association of Comammox
713 *Nitrospira* and Anammox bacteria. *bioRxiv* doi:10.1101/2020.10.12.336248.
- 714 27. Wang X, Wang S, Jiang Y, Zhou J, Han C, Zhu G. 2020. Comammox bacterial
715 abundance, activity, and contribution in agricultural rhizosphere soils. *Sci Total Environ*
716 727:138563.
- 717 28. He S, Li Y, Mu H, Zhao Z, Wang J, Liu S, Sun Z, Zheng M. 2021. Ammonium
718 concentration determines differential growth of comammox and canonical ammonia-
719 oxidizing prokaryotes in soil microcosms. *Applied Soil Ecology* 157.
- 720 29. Shao YH, Wu JH. 2021. Comammox *Nitrospira* Species Dominate in an Efficient Partial
721 Nitrification-Anammox Bioreactor for Treating Ammonium at Low Loadings. *Environ*
722 *Sci Technol* 55:2087-2098.

- 723 30. Yang Y, Daims H, Liu Y, Herbold CW, Pjevac P, Lin J-G, Li M, Gu J-D. 2020. Activity
724 and Metabolic Versatility of Complete Ammonia Oxidizers in Full-Scale Wastewater
725 Treatment Systems. *mBio* 11:e03175-19.
- 726 31. Gonzalez-Martinez A, Rodriguez-Sanchez A, van Loosdrecht MCM, Gonzalez-Lopez J,
727 Vahala R. 2016. Detection of comammox bacteria in full-scale wastewater treatment
728 bioreactors using tag-454-pyrosequencing. *Environ Sci Pollut Res Int* 23:25501-25511.
- 729 32. Roots P, Wang Y, Rosenthal AF, Griffin JS, Sabba F, Petrovich M, Yang F, Kozak JA,
730 Zhang H, Wells GF. 2019. Comammox Nitrospira are the dominant ammonia oxidizers
731 in a mainstream low dissolved oxygen nitrification reactor. *Water Res* 157:396-405.
- 732 33. Tatari K, Musovic S, Gulay A, Dechesne A, Albrechtsen HJ, Smets BF. 2017. Density
733 and distribution of nitrifying guilds in rapid sand filters for drinking water production:
734 Dominance of Nitrospira spp. *Water Res* 127:239-248.
- 735 34. Poghosyan L, Koch H, Frank J, van Kessel M, Cremers G, van Alen T, Jetten MSM, Op
736 den Camp HJM, Lucker S. 2020. Metagenomic profiling of ammonia- and methane-
737 oxidizing microorganisms in two sequential rapid sand filters. *Water Res* 185:116288.
- 738 35. Prosser JI, Nicol GW. 2012. Archaeal and bacterial ammonia-oxidisers in soil: the quest
739 for niche specialisation and differentiation. *Trends Microbiol* 20:523-31.
- 740 36. Shi X, Hu H-W, Wang J, He J-Z, Zheng C, Wan X, Huang Z. 2018. Niche separation of
741 comammox Nitrospira and canonical ammonia oxidizers in an acidic subtropical forest
742 soil under long-term nitrogen deposition. *Soil Biology and Biochemistry* 126:114-122.
- 743 37. Koch H, Lucker S, Albertsen M, Kitzinger K, Herbold C, Spieck E, Nielsen PH, Wagner
744 M, Daims H. 2015. Expanded metabolic versatility of ubiquitous nitrite-oxidizing
745 bacteria from the genus Nitrospira. *Proc Natl Acad Sci U S A* 112:11371-6.
- 746 38. Palomo A, Pedersen AG, Fowler SJ, Dechesne A, Sicheritz-Ponten T, Smets BF. 2018.
747 Comparative genomics sheds light on niche differentiation and the evolutionary history
748 of comammox Nitrospira. *ISME J* 12:1779-1793.
- 749 39. Bowers RM, Kyrpides NC, Stepanauskas R, Harmon-Smith M, Doud D, Reddy TBK,
750 Schulz F, Jarett J, Rivers AR, Eloie-Fadrosch EA, Tringe SG, Ivanova NN, Copeland A,
751 Clum A, Becraft ED, Malmstrom RR, Birren B, Podar M, Bork P, Weinstock GM,
752 Garrity GM, Dodsworth JA, Yooseph S, Sutton G, Glockner FO, Gilbert JA, Nelson WC,
753 Hallam SJ, Jungbluth SP, Ettema TJG, Tighe S, Konstantinidis KT, Liu WT, Baker BJ,
754 Rattei T, Eisen JA, Hedlund B, McMahon KD, Fierer N, Knight R, Finn R, Cochrane G,
755 Karsch-Mizrachi I, Tyson GW, Rinke C, Genome Standards C, Lapidus A, Meyer F,
756 Yilmaz P, Parks DH, et al. 2017. Minimum information about a single amplified genome
757 (MISAG) and a metagenome-assembled genome (MIMAG) of bacteria and archaea. *Nat*
758 *Biotechnol* 35:725-731.
- 759 40. Parks DH, Rinke C, Chuvochina M, Chaumeil PA, Woodcroft BJ, Evans PN, Hugenholtz
760 P, Tyson GW. 2017. Recovery of nearly 8,000 metagenome-assembled genomes
761 substantially expands the tree of life. *Nat Microbiol* 2:1533-1542.
- 762 41. Gulay A, Musovic S, Albrechtsen HJ, Al-Soud WA, Sorensen SJ, Smets BF. 2016.
763 Ecological patterns, diversity and core taxa of microbial communities in groundwater-fed
764 rapid gravity filters. *ISME J* 10:2209-22.
- 765 42. Bollmann A, French E, Laanbroek HJ. 2011. Isolation, cultivation, and characterization
766 of ammonia-oxidizing bacteria and archaea adapted to low ammonium concentrations.
767 *Methods Enzymol* 486:55-88.

- 768 43. Sedlacek CJ, McGowan B, Suwa Y, Sayavedra-Soto L, Laanbroek HJ, Stein LY, Norton
769 JM, Klotz MG, Bollmann A. 2019. A Physiological and Genomic Comparison of
770 Nitrosomonas Cluster 6a and 7 Ammonia-Oxidizing Bacteria. *Microb Ecol* 78:985-994.
- 771 44. Spasov E, Tsuji JM, Hug LA, Doxey AC, Sauder LA, Parker WJ, Neufeld JD. 2020.
772 High functional diversity among Nitrospira populations that dominate rotating biological
773 contactor microbial communities in a municipal wastewater treatment plant. *ISME J*
774 14:1857-1872.
- 775 45. Koops H-P, Purkhold U, Pommerening-Röser A, Timmermann G, Wagner M. 2006. The
776 Lithoautotrophic Ammonia-Oxidizing Bacteria, p 778-811, *The Prokaryotes*
777 doi:10.1007/0-387-30745-1_36.
- 778 46. Martens-Habbena W, Berube PM, Urakawa H, de la Torre JR, Stahl DA. 2009. Ammonia
779 oxidation kinetics determine niche separation of nitrifying Archaea and Bacteria. *Nature*
780 461:976-9.
- 781 47. Hermansson A, Lindgren PE. 2001. Quantification of ammonia-oxidizing bacteria in
782 arable soil by real-time PCR. *Appl Environ Microbiol* 67:972-6.
- 783 48. Graham DW, Knapp CW, Van Vleck ES, Bloor K, Lane TB, Graham CE. 2007.
784 Experimental demonstration of chaotic instability in biological nitrification. *ISME J*
785 1:385-93.
- 786 49. Caporaso JG, Lauber CL, Walters WA, Berg-Lyons D, Lozupone CA, Turnbaugh PJ,
787 Fierer N, Knight R. 2011. Global patterns of 16S rRNA diversity at a depth of millions of
788 sequences per sample. *Proc Natl Acad Sci U S A* 108 Suppl 1:4516-22.
- 789 50. Chen S, Zhou Y, Chen Y, Gu J. 2018. fastp: an ultra-fast all-in-one FASTQ preprocessor.
790 *Bioinformatics* 34:i884-i890.
- 791 51. Li H, Durbin R. 2009. Fast and accurate short read alignment with Burrows-Wheeler
792 transform. *Bioinformatics* 25:1754-60.
- 793 52. Li H, Handsaker B, Wysoker A, Fennell T, Ruan J, Homer N, Marth G, Abecasis G,
794 Durbin R, Genome Project Data Processing S. 2009. The Sequence Alignment/Map
795 format and SAMtools. *Bioinformatics* 25:2078-9.
- 796 53. Quinlan AR, Hall IM. 2010. BEDTools: a flexible suite of utilities for comparing
797 genomic features. *Bioinformatics* 26:841-2.
- 798 54. Gruber-Vodicka HR, Seah BKB, Pruesse E. 2020. phyloFlash: Rapid Small-Subunit
799 rRNA Profiling and Targeted Assembly from Metagenomes. *mSystems* 5.
- 800 55. Pruesse E, Quast C, Knittel K, Fuchs BM, Ludwig W, Peplies J, Glockner FO. 2007.
801 SILVA: a comprehensive online resource for quality checked and aligned ribosomal
802 RNA sequence data compatible with ARB. *Nucleic Acids Res* 35:7188-96.
- 803 56. Rognes T, Flouri T, Nichols B, Quince C, Mahe F. 2016. VSEARCH: a versatile open
804 source tool for metagenomics. *PeerJ* 4:e2584.
- 805 57. Edgar RC. 2004. MUSCLE: a multiple sequence alignment method with reduced time
806 and space complexity. *BMC Bioinformatics* 5:113.
- 807 58. Nguyen LT, Schmidt HA, von Haeseler A, Minh BQ. 2015. IQ-TREE: a fast and
808 effective stochastic algorithm for estimating maximum-likelihood phylogenies. *Mol Biol*
809 *Evol* 32:268-74.
- 810 59. Kalyaanamoorthy S, Minh BQ, Wong TKF, von Haeseler A, Jermiin LS. 2017.
811 ModelFinder: fast model selection for accurate phylogenetic estimates. *Nat Methods*
812 14:587-589.

- 813 60. Nurk S, Meleshko D, Korobeynikov A, Pevzner PA. 2017. metaSPAdes: a new versatile
814 metagenomic assembler. *Genome Res* 27:824-834.
- 815 61. Gurevich A, Saveliev V, Vyahhi N, Tesler G. 2013. QUAST: quality assessment tool for
816 genome assemblies. *Bioinformatics* 29:1072-5.
- 817 62. Hyatt D, Chen GL, Locascio PF, Land ML, Larimer FW, Hauser LJ. 2010. Prodigal:
818 prokaryotic gene recognition and translation initiation site identification. *BMC*
819 *Bioinformatics* 11:119.
- 820 63. Hiroyuki Ogata SG, Kazushige Sato, Wataru Fujibuchi, Hidemasa Bono and Minoru
821 Kanehisa. 1999. KEGG: Kyoto Encyclopedia of Genes and Genomes. *Nucleic Acids*
822 *Research* 27.
- 823 64. Aramaki T, Blanc-Mathieu R, Endo H, Ohkubo K, Kanehisa M, Goto S, Ogata H. 2020.
824 KofamKOALA: KEGG Ortholog assignment based on profile HMM and adaptive score
825 threshold. *Bioinformatics* 36:2251-2252.
- 826 65. Menzel P, Ng KL, Krogh A. 2016. Fast and sensitive taxonomic classification for
827 metagenomics with Kaiju. *Nat Commun* 7:11257.
- 828 66. Eren AM, Esen OC, Quince C, Vineis JH, Morrison HG, Sogin ML, Delmont TO. 2015.
829 Anvi'o: an advanced analysis and visualization platform for 'omics data. *PeerJ* 3:e1319.
- 830 67. Alneberg J, Bjarnason BS, de Bruijn I, Schirmer M, Quick J, Ijaz UZ, Lahti L, Loman
831 NJ, Andersson AF, Quince C. 2014. Binning metagenomic contigs by coverage and
832 composition. *Nat Methods* 11:1144-6.
- 833 68. Kang DD, Li F, Kirton E, Thomas A, Egan R, An H, Wang Z. 2019. MetaBAT 2: an
834 adaptive binning algorithm for robust and efficient genome reconstruction from
835 metagenome assemblies. *PeerJ* 7:e7359.
- 836 69. Wu YW, Simmons BA, Singer SW. 2016. MaxBin 2.0: an automated binning algorithm
837 to recover genomes from multiple metagenomic datasets. *Bioinformatics* 32:605-7.
- 838 70. Sieber CMK, Probst AJ, Sharrar A, Thomas BC, Hess M, Tringe SG, Banfield JF. 2018.
839 Recovery of genomes from metagenomes via a dereplication, aggregation and scoring
840 strategy. *Nat Microbiol* 3:836-843.
- 841 71. Parks DH, Imelfort M, Skennerton CT, Hugenholtz P, Tyson GW. 2015. CheckM:
842 assessing the quality of microbial genomes recovered from isolates, single cells, and
843 metagenomes. *Genome Res* 25:1043-55.
- 844 72. Chaumeil PA, Mussig AJ, Hugenholtz P, Parks DH. 2019. GTDB-Tk: a toolkit to classify
845 genomes with the Genome Taxonomy Database. *Bioinformatics*
846 doi:10.1093/bioinformatics/btz848.
- 847 73. Seemann T. 2014. Prokka: rapid prokaryotic genome annotation. *Bioinformatics*
848 30:2068-9.
- 849 74. Na SI, Kim YO, Yoon SH, Ha SM, Baek I, Chun J. 2018. UBCG: Up-to-date bacterial
850 core gene set and pipeline for phylogenomic tree reconstruction. *J Microbiol* 56:280-285.
- 851 75. Letunic I, Bork P. 2019. Interactive Tree Of Life (iTOL) v4: recent updates and new
852 developments. *Nucleic Acids Res* 47:W256-W259.
- 853 76. Jain C, Rodriguez RL, Phillippy AM, Konstantinidis KT, Aluru S. 2018. High throughput
854 ANI analysis of 90K prokaryotic genomes reveals clear species boundaries. *Nat Commun*
855 9:5114.
856
857
858

859

860 **List of Figures.**

861

862 **Figure 1:** A) Proportion of SSU reads mapping to the SILVA SSU NR99 database (version 138.1)
863 from the inocula and treated samples at weeks four and eight. The community primarily consisted
864 of Gammaproteobacteria, Alphaproteobacteria and Nitrospirota. Proteobacteria is broken down
865 by classes, Alphaproteobacteria and Gammaproteobacteria, though a small portion of
866 Proteobacteria reads could not be classified further. B) Taxonomic classification of genes for
867 nitrogen biotransformation present in the metagenome at the phyla level with Proteobacteria
868 presented by classes, Alphaproteobacteria and Gammaproteobacteria. C and D) Phylogenetic
869 placement of amoA-pmoA like sequences (C), and nxrA sequences (D) detected in the
870 metagenomes. Both maximum likelihood trees were constructed based alignments of protein
871 sequences of the respective genes. Sequences identified in this study are colored according to their
872 phylogenetic placement (red, green, blue and orange) while references are black. AOB = ammonia
873 oxidizing bacteria, MOB = methane oxidizing bacteria.

874

875 **Figure 2:** Phylogenomic tree for Nitrospira MAGs (blue and green) obtained in this study and 32
876 reference genomes (black). Blue label = comammox, green label = NOB. Branch colors represent
877 different Nitrospira sublineages. Two Leptospirillum reference genomes were used as the outgroup
878 for maximum likelihood tree construction. B) Maximum likelihood tree based on ammonia
879 monooxygenase subunit A (amoA) sequences from comammox-Nitrospira. C) Maximum
880 likelihood tree based on hydroxylamine oxidoreductase (hao) sequences of comammox-Nitrospira.
881 For B and C blue labels represent amoA/hao gene sequences found in comammox MAGs from
882 this study, while black labels are reference sequences. Environment of origin is denoted with

883 colored squares to the left of each tree. amoA and hao protein sequences from Nitrosomonas
884 europaea and Nitrosomonas oligotropha were used as the outgroup for comammox trees in B and
885 C, respectively. D) Phylogenomic tree for strict AOB MAGs (yellow) obtained in this study and
886 10 Nitrosomonas reference genomes (black). Three Nitrospira genomes were used as the
887 outgroup.

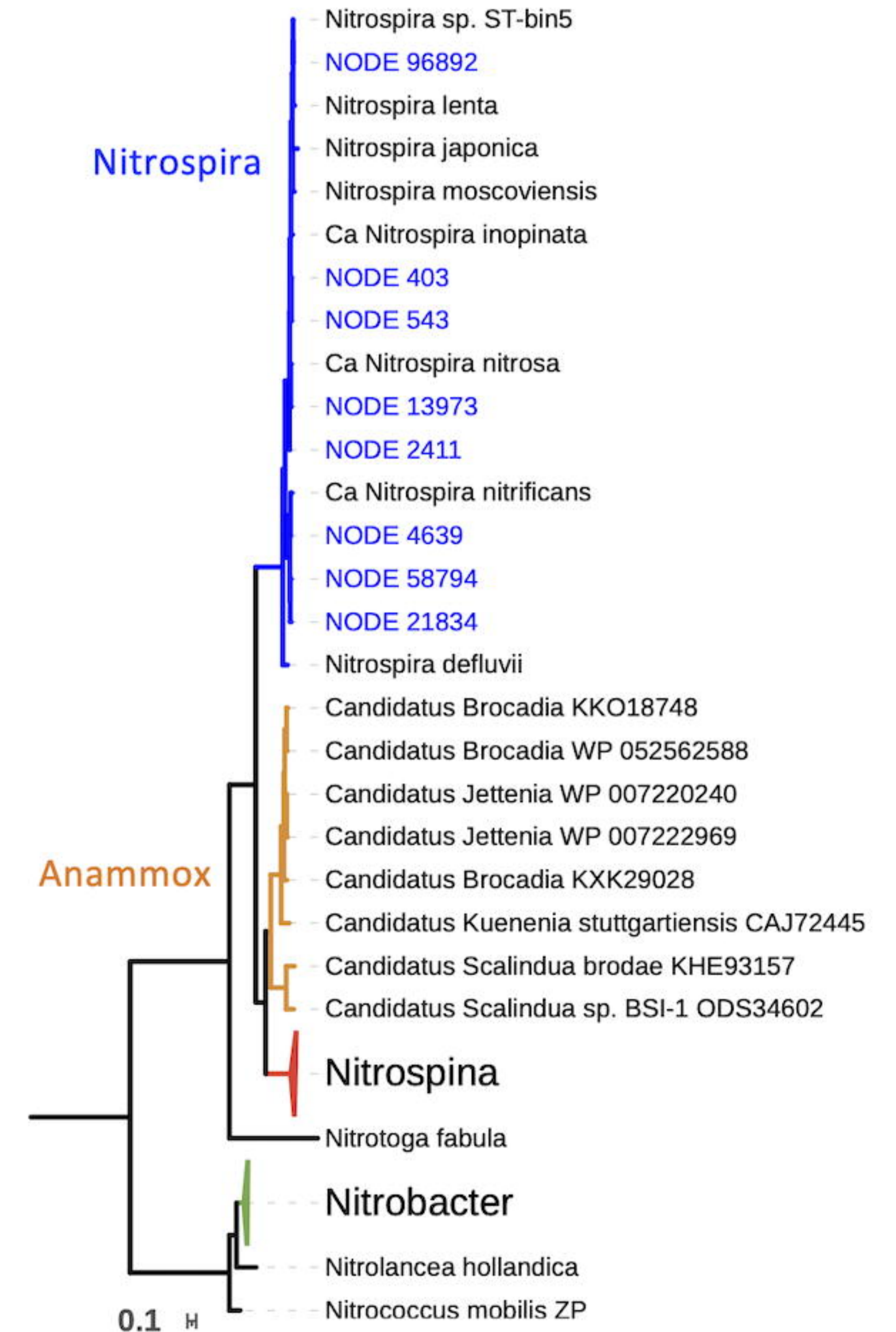
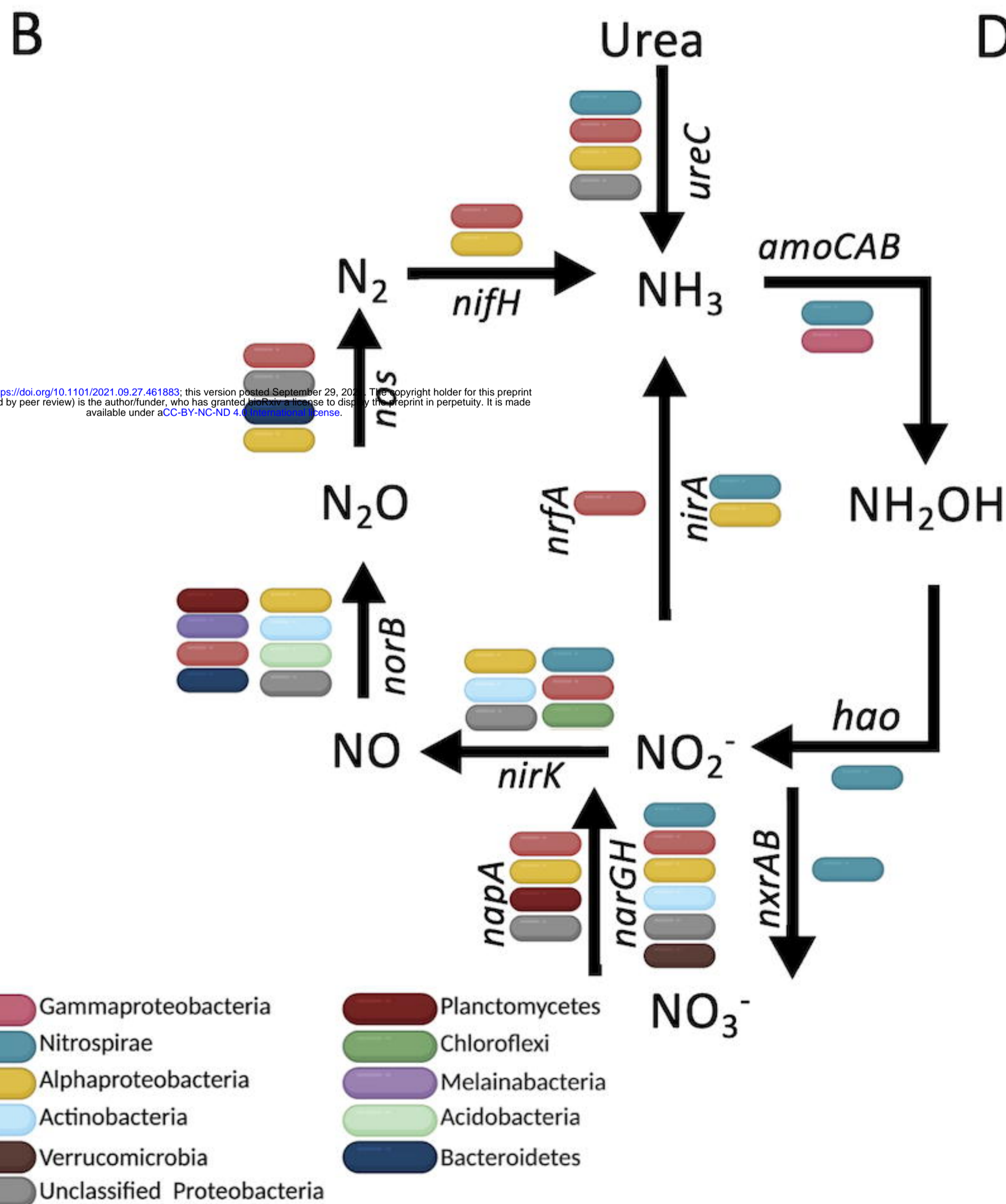
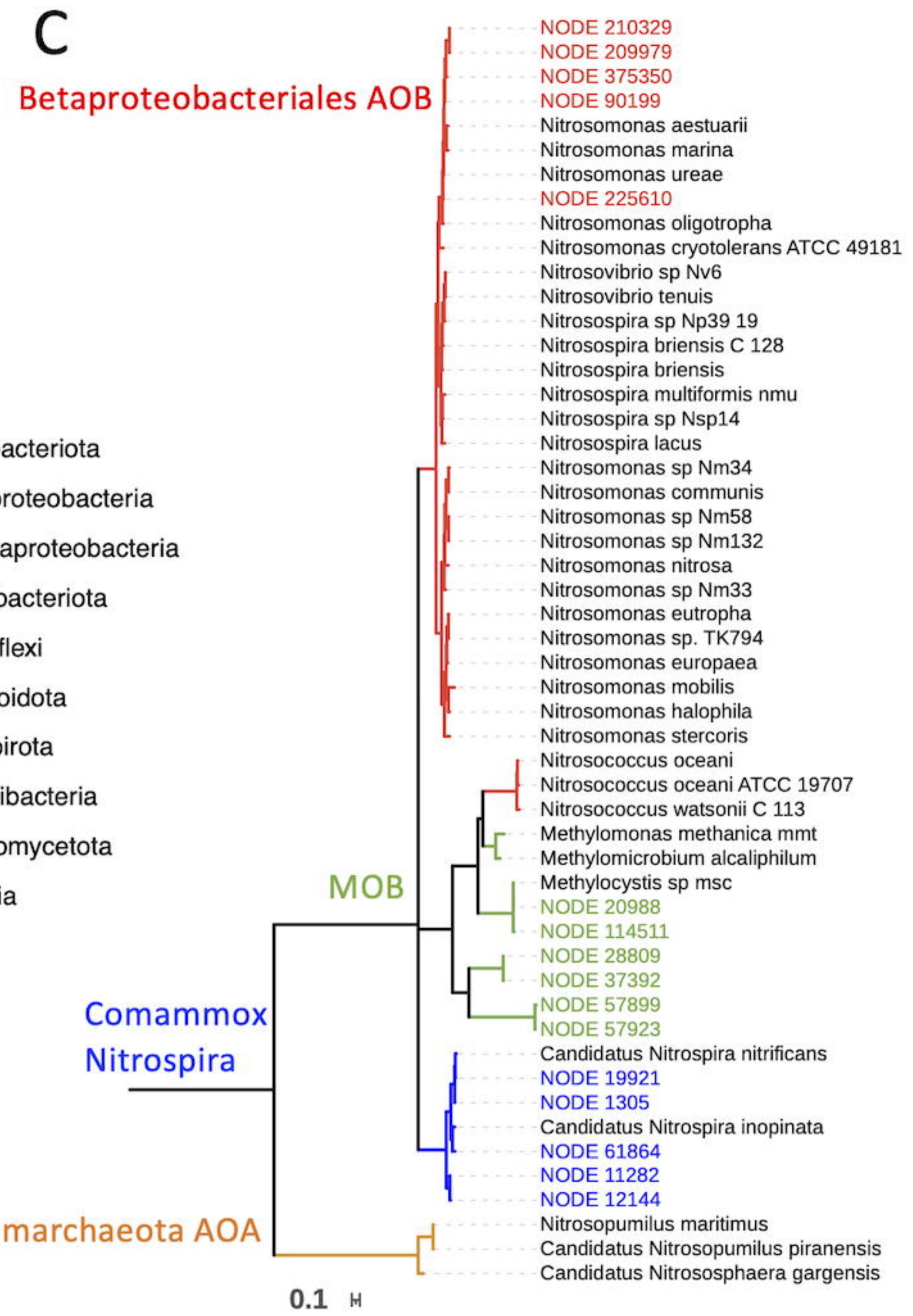
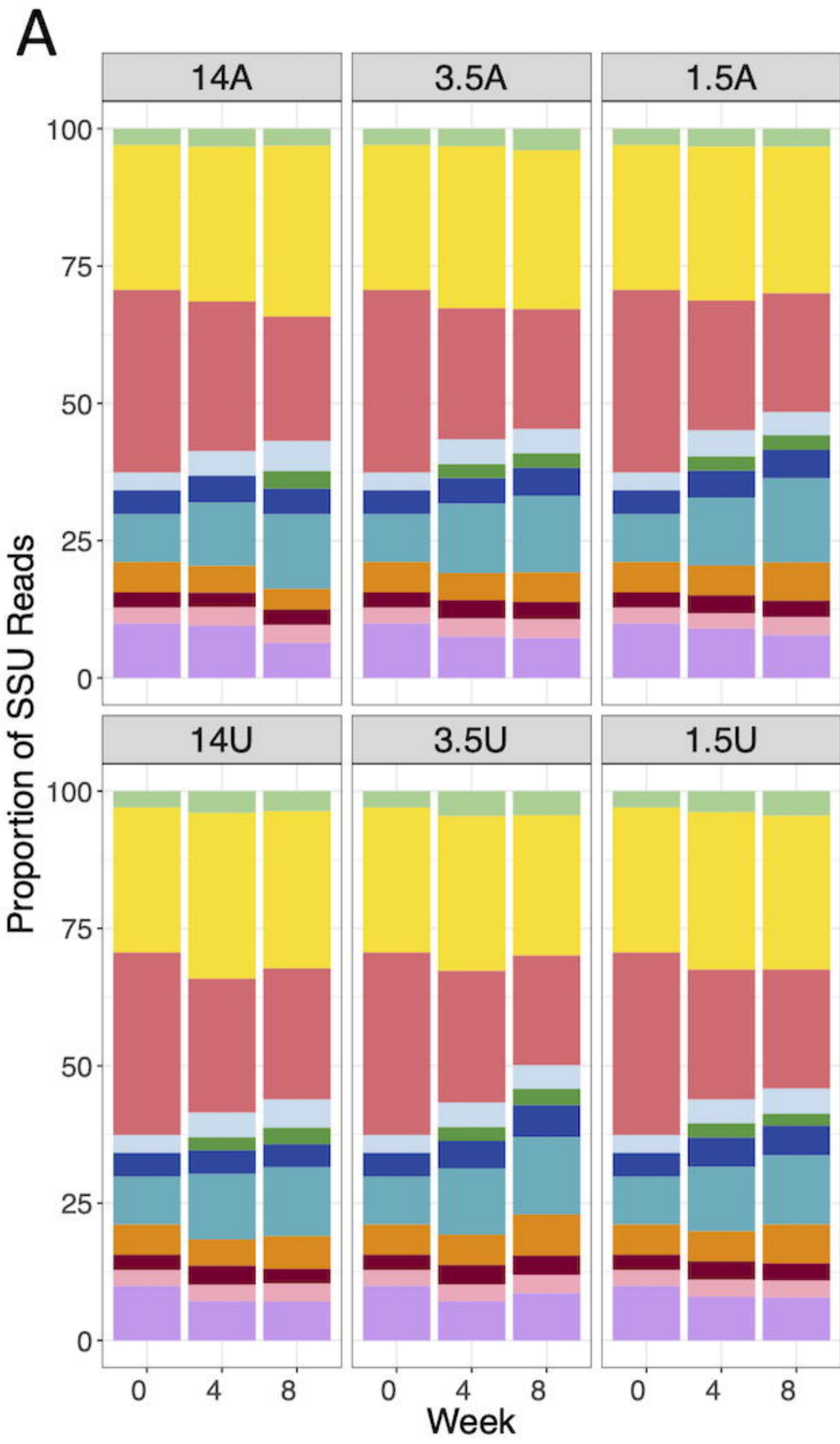
888

889 **Figure 3:** A) The relative abundance of comammox bacteria (blue) and strict AOB (red) as a
890 proportion of all ammonia oxidizing microorganisms calculated using copy number of 16S rRNA
891 and amoB genes of strict AOB and comammox bacteria, respectively and dividing by the
892 combined copy number to represent total AOM for each time point. Data points are the average
893 ratio between duplicate samples. B) Relative abundance of comammox bacteria (blue), Nitrospira-
894 NOB (orange) and strict AOB (red) as a proportion of total bacteria using the ratio of copy number
895 of the respective nitrifier genes to copy number of total bacteria averaged between duplicate
896 samples. Initial abundances of comammox bacteria, Nitrospira-NOB, and strict AOB were 1.2, 1.7
897 and 0.9% of total bacteria, respectively. Panels display relative abundances of the nitrifiers subject
898 to varying nitrogen amendments. C) Reads per kilobase million (RPKM) calculated for all MAGs
899 identifying as comammox bacteria (blue), Nitrospira-NOB (orange) and strict AOB (red) at
900 selected time points.

901

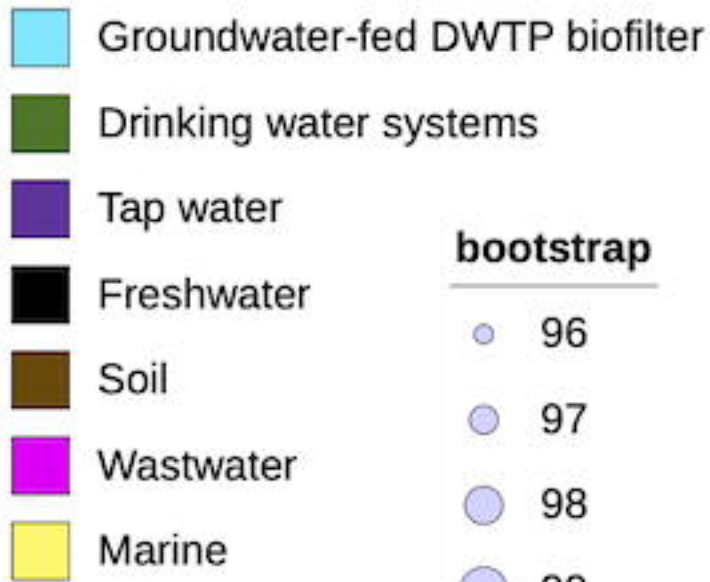
902 **Figure 4:** A) Significant positive correlation between changes in AOB concentration and that of
903 Nitrospira-NOB as a proportion of total bacteria were found in most treatments except low
904 ammonia (1.5A). B) Negative associations between changes in comammox bacteria concentration
905 and that of Nitrospira-NOB as a proportion of total bacteria existed in ammonia amendments with

906 statistically significance detected in 3.5A and 1.5A while no association existed in urea
907 amendments.
908

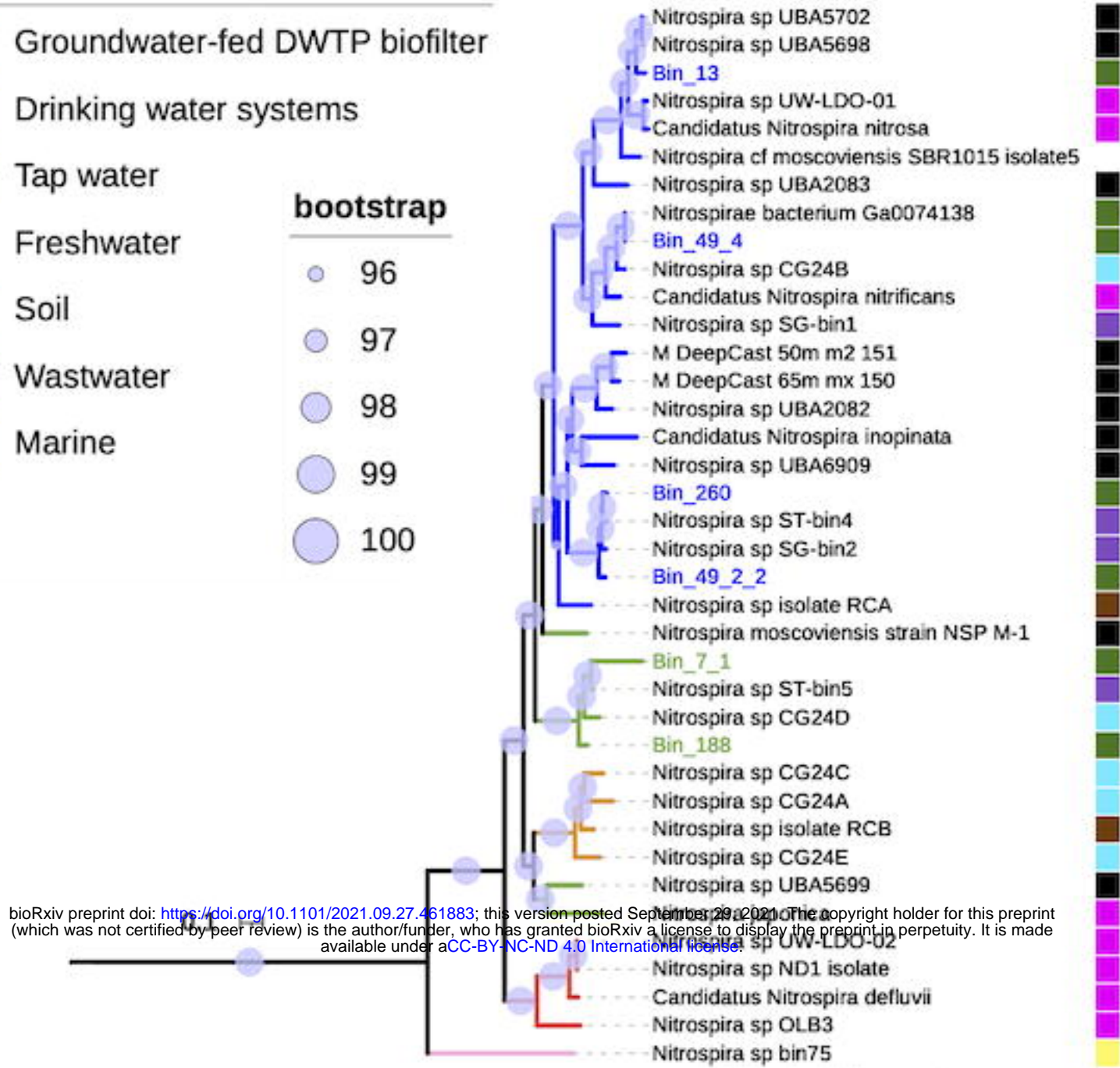
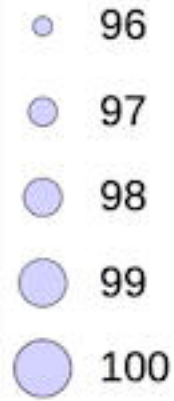


A

Environment of Origin

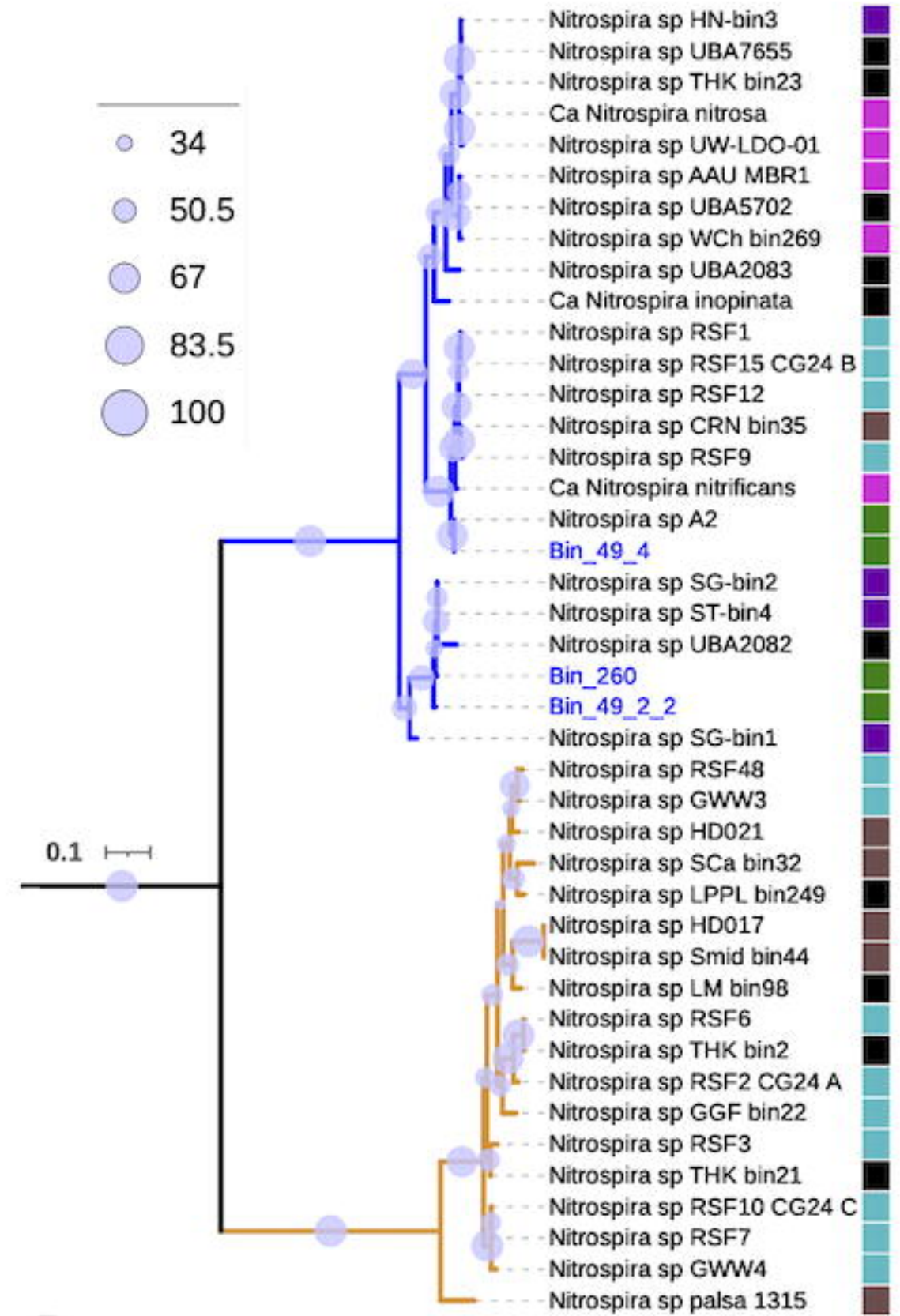


bootstrap

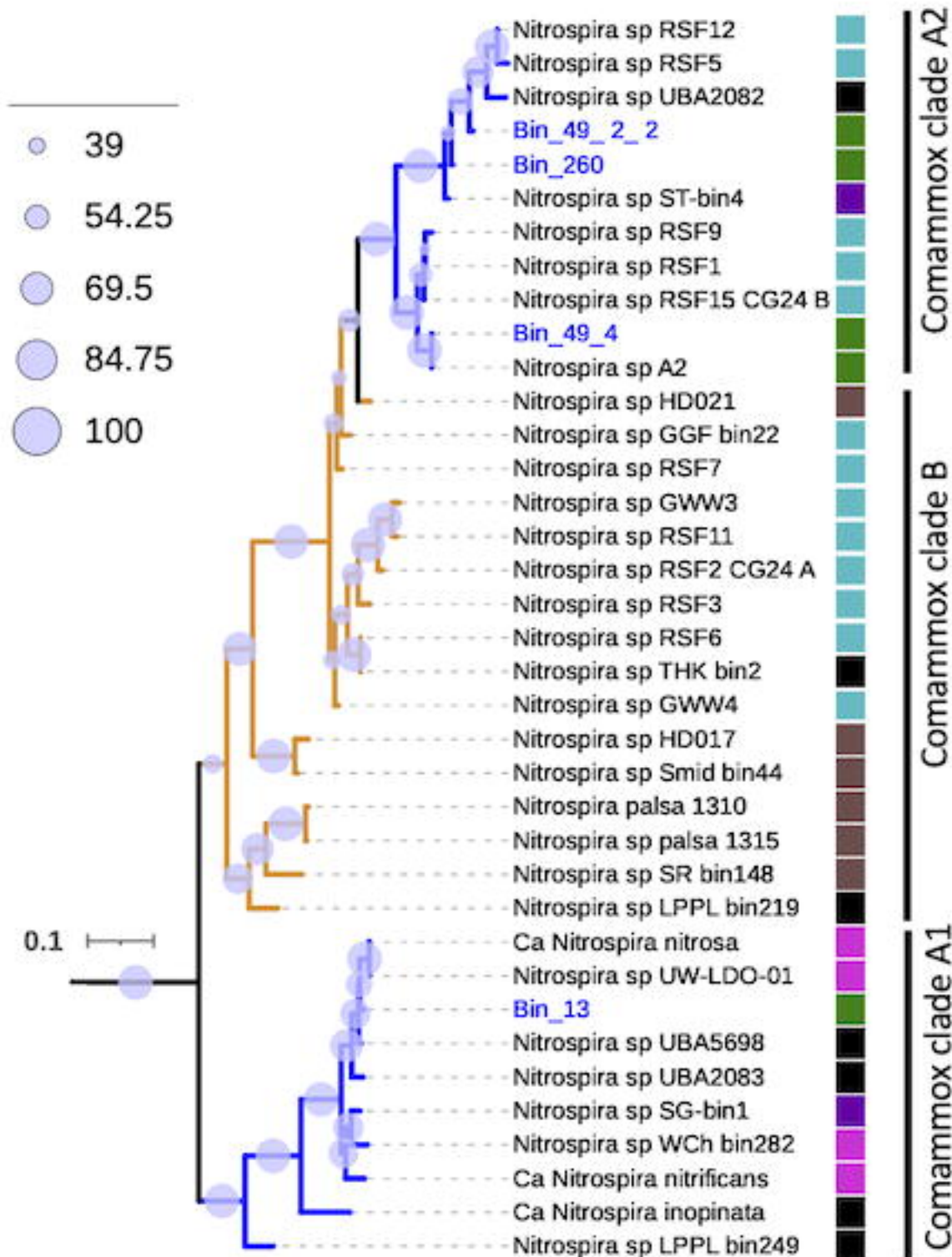


bioRxiv preprint doi: <https://doi.org/10.1101/2021.09.27.461883>; this version posted September 29, 2021. The copyright holder for this preprint (which was not certified by peer review) is the author/funder, who has granted bioRxiv a license to display the preprint in perpetuity. It is made available under aCC-BY-NC-ND 4.0 International license.

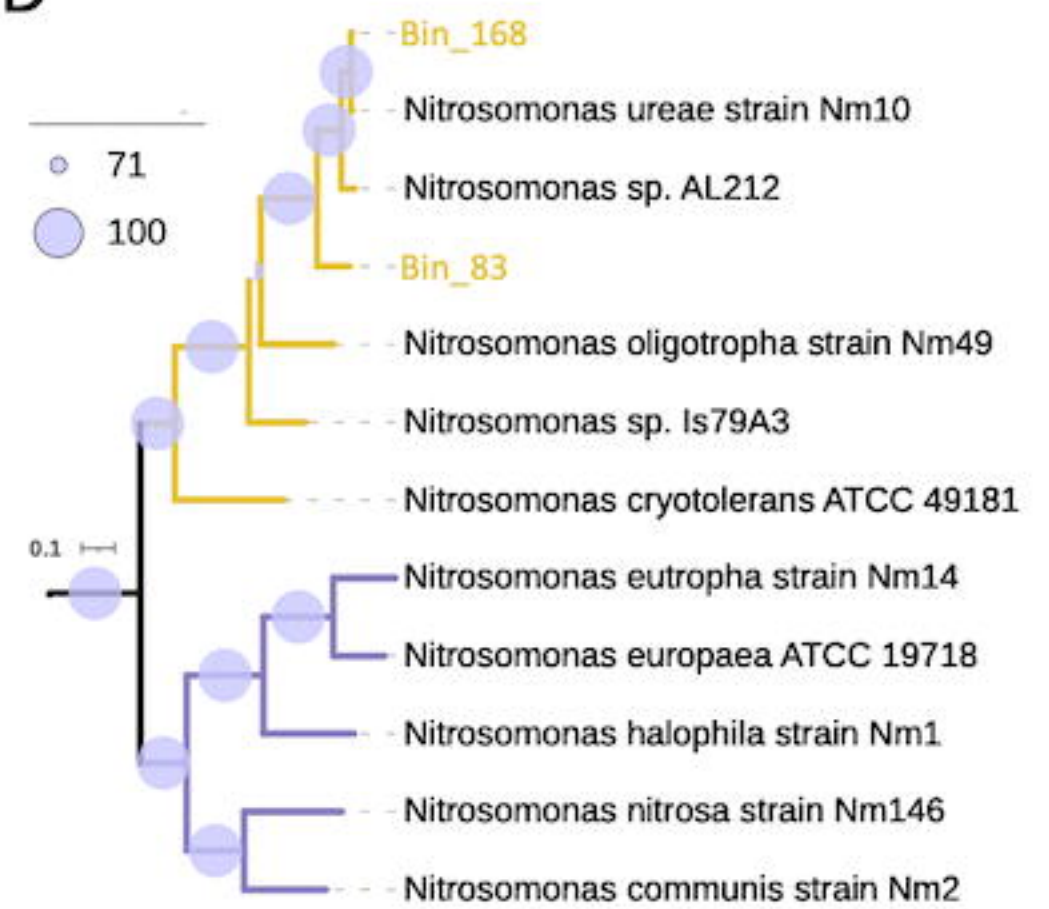
B



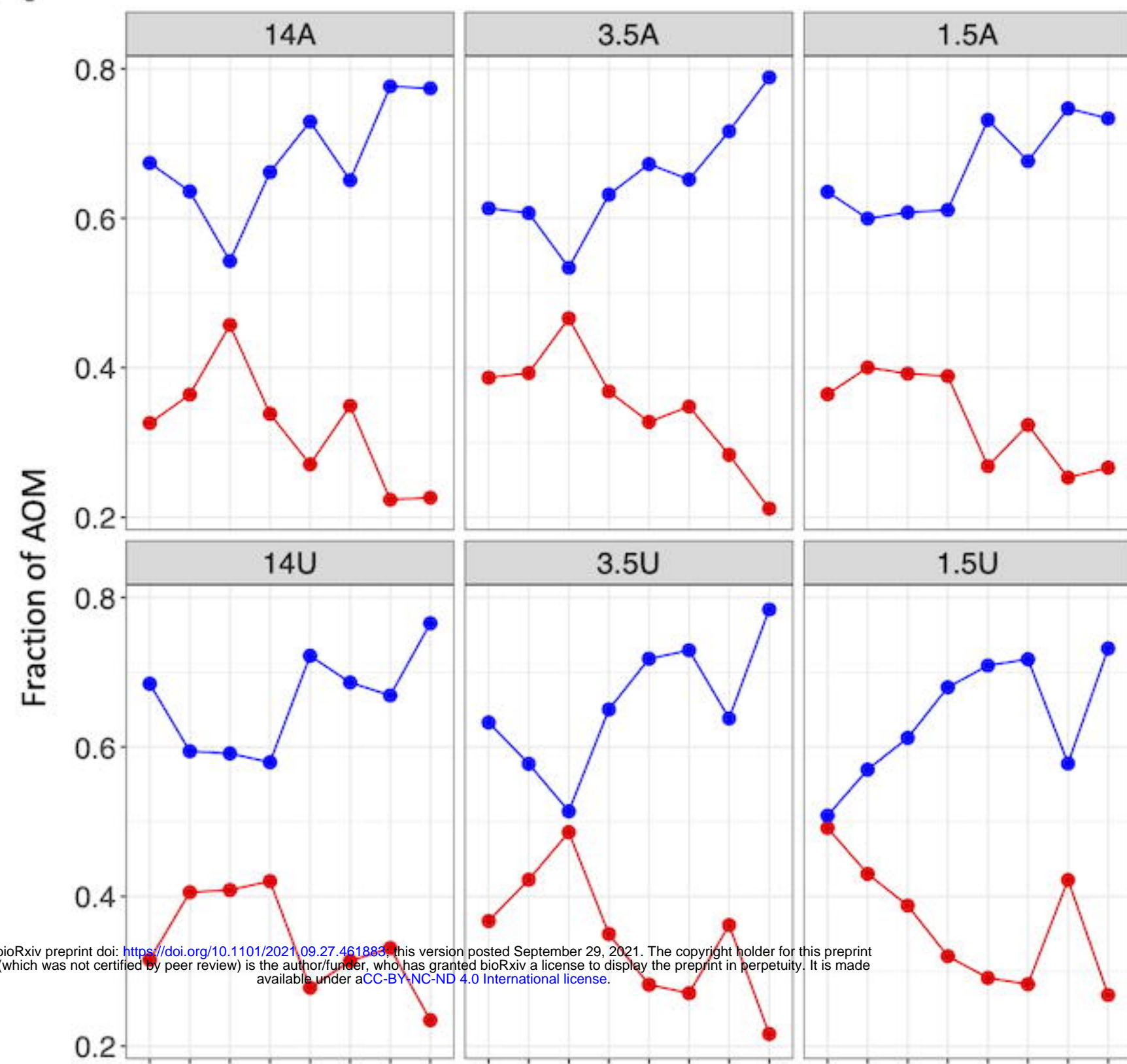
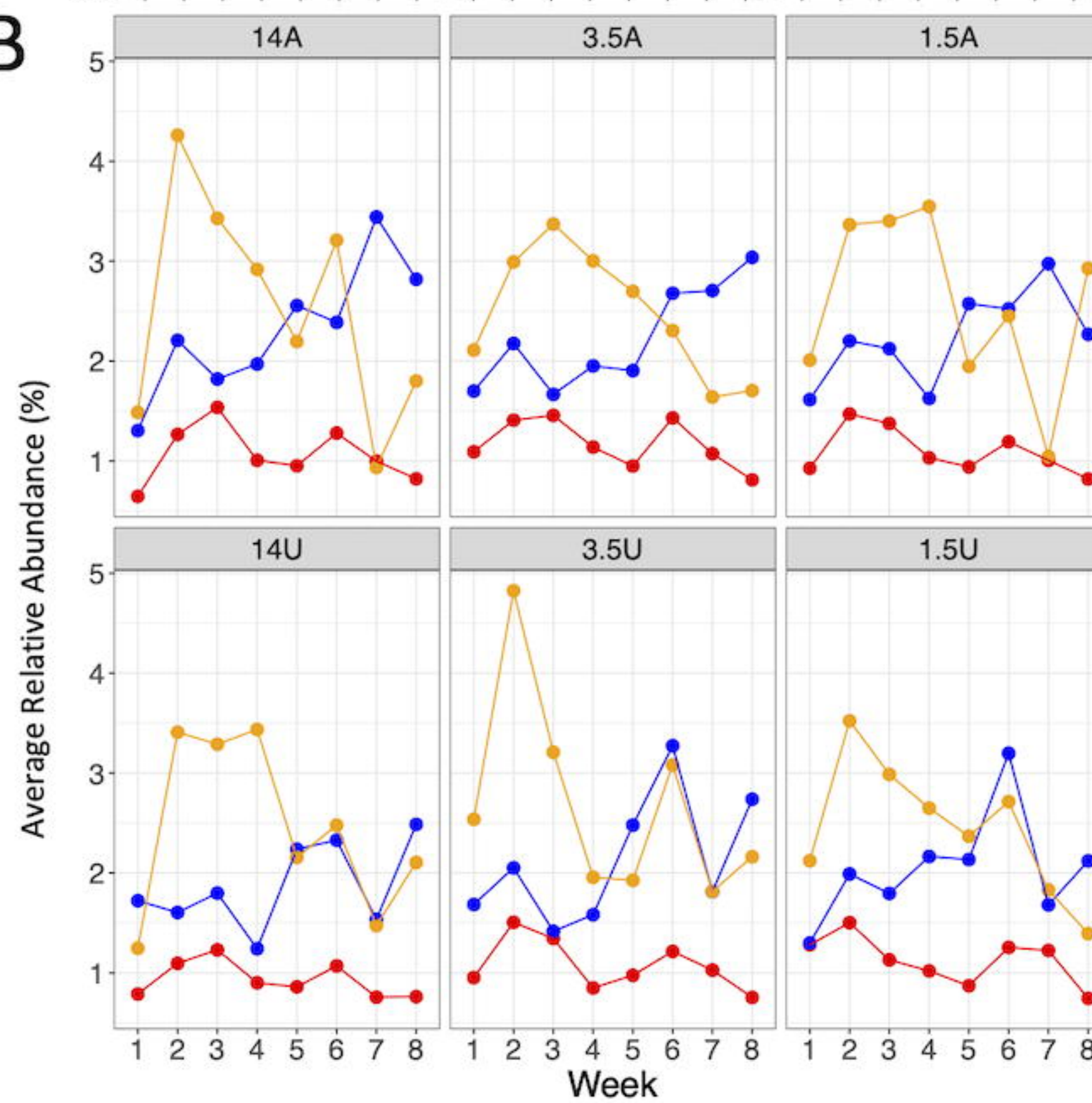
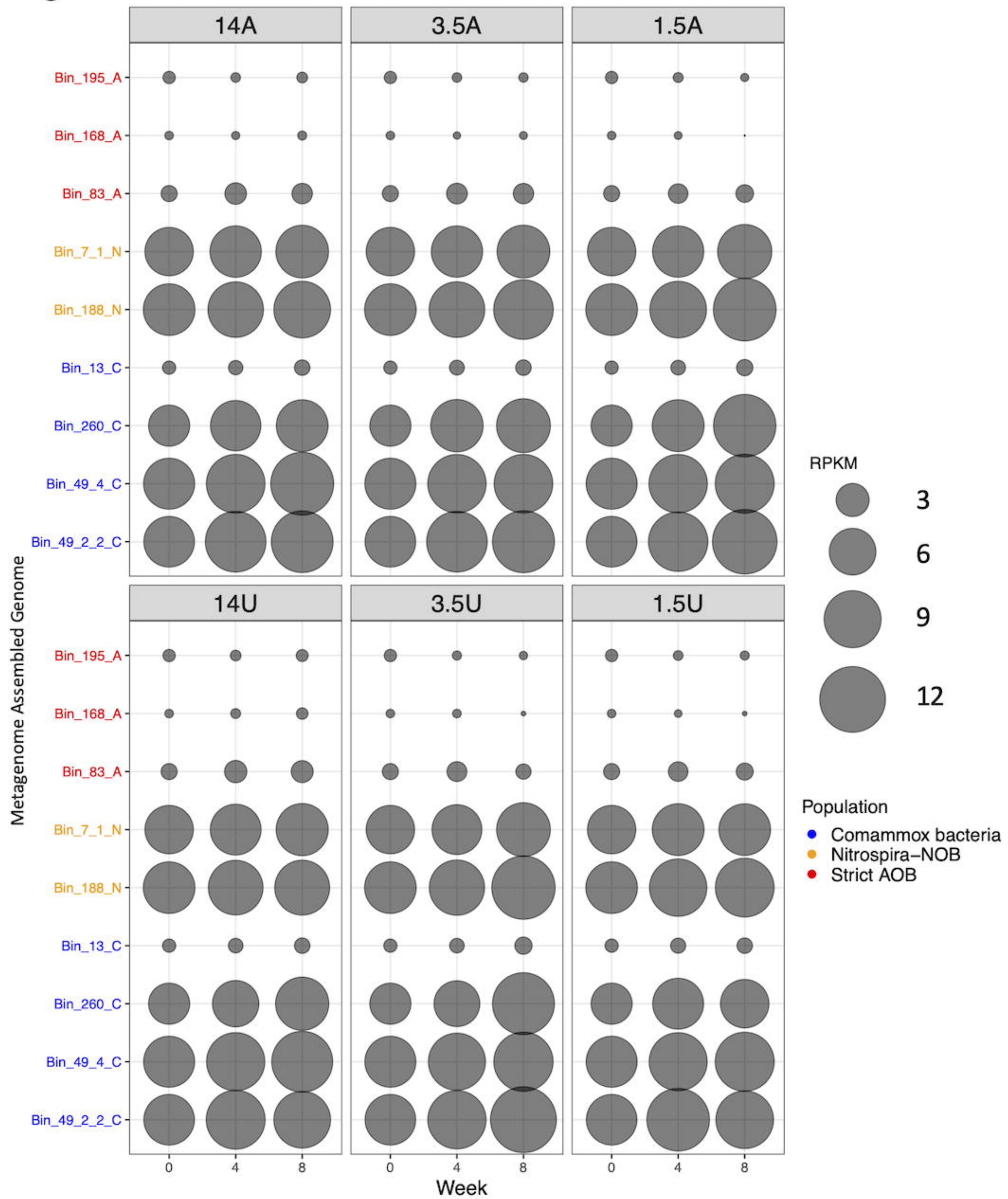
C

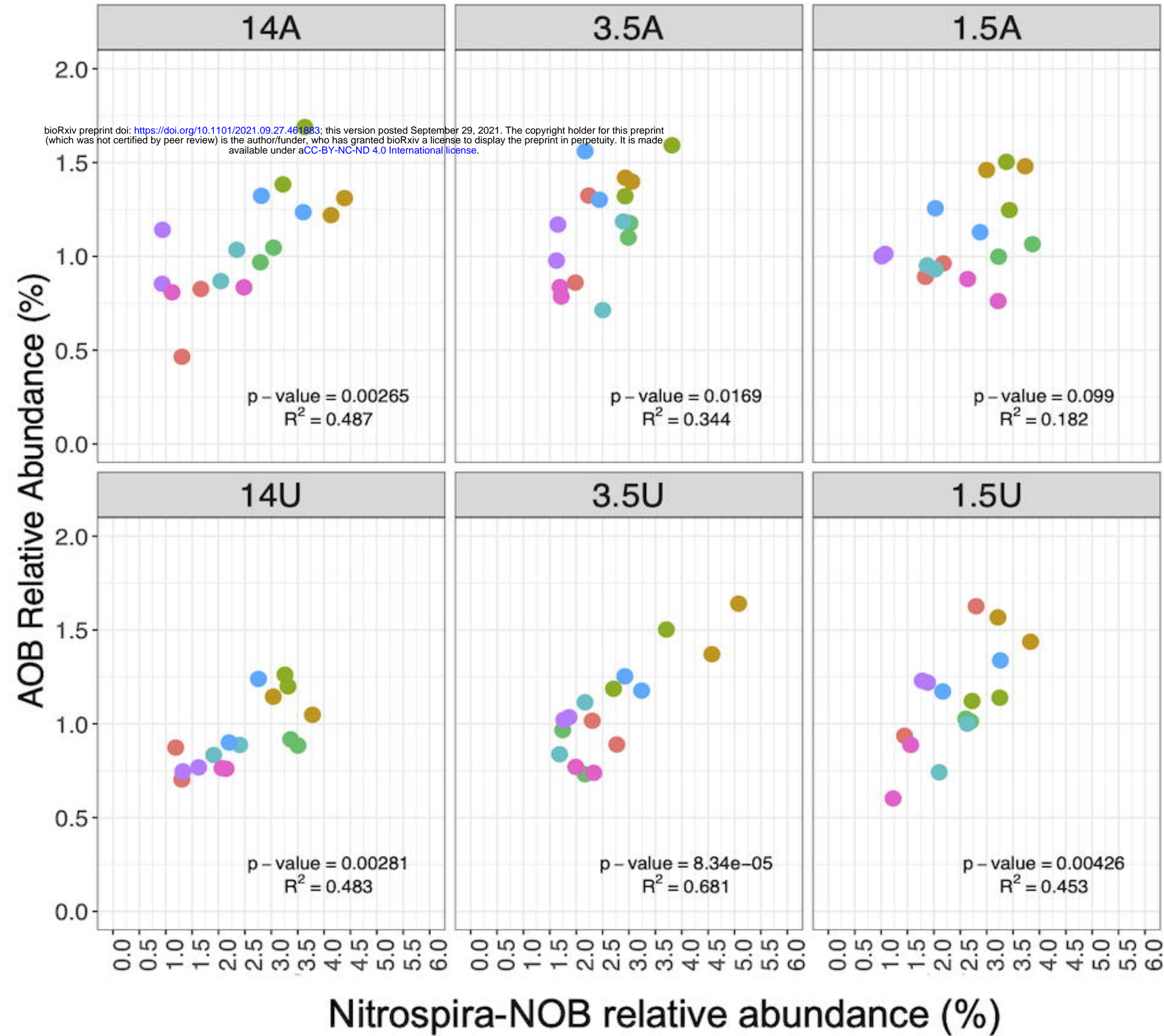


D



Sublineage II clade A comammox-*Nitrospira*
Sublineage II *Nitrospira*-NOB
Sublineage II clade B comammox-*Nitrospira*
Sublineage I *Nitrospira*-NOB
Sublineage IV *Nitrospira*-NOB
Nitrosomonas cluster 6a
Nitrosomonas cluster 7

A**B****C**

A**B**